Habitat-specificity in SAR11 is associated with a handful of genes under high selection

Sarah J. Tucker[1,2,3,4,5], Kelle C. Freel[1], A. Murat Eren[3,4,5,6,7,#,*], Michael S. Rappé[1,#,*]

[1]Hawai'i Institute of Marine Biology, School of Ocean and Earth Science and Technology, University of Hawai'i at Mānoa, Kāne'ohe, HI 96744, USA; [2]Marine Biology Graduate Program, University of Hawai‘i at Mānoa, Honolulu, Hawai‘i, United States; [3]Josephine Bay Paul Center for Comparative Molecular Biology and Evolution, Marine Biological Laboratory, Woods Hole, MA 02543, USA; [4]Helmholtz Institute for Functional Marine Biodiversity, 26129 Oldenburg, Germany; [5]Alfred Wegener Institute, Helmholtz Centre for Polar and Marine Research, 27570 Bremerhaven, Germany; [6]Institute for Chemistry and Biology of the Marine Environment, University of Oldenburg, 26129 Oldenburg, Germany; [7]Max Planck Institute for Marine Microbiology, 28359 Bremen, Germany

[#]Co-senior Authors

*Corresponding Authors. Email: meren@hifmb.de, rappe@hawaii.edu

Running Title: Ecotype differentiation in SAR11

Abstract

The order *Pelagibacterales* (SAR11) is the most abundant group of heterotrophic bacteria in the global surface ocean, where individual sublineages likely play distinct roles in oceanic biogeochemical cycles. Yet, understanding the determinants of niche partitioning within SAR11 has been a formidable challenge due to the high genetic diversity within individual SAR11 sublineages and the limited availability of high-quality genomes from both cultivation and metagenomic reconstruction. Here, we take advantage of 71 new SAR11 genomes from strains we isolated from the tropical Pacific Ocean to evaluate the distribution of metabolic traits across the *Pelagibacteraceae,* a recently classified family within the order *Pelagibacterales* encompassing subgroups Ia and Ib. Our analyses of metagenomes generated from stations where the strains were isolated reveals distinct habitat preferences across SAR11 genera for coastal or offshore environments, and subtle but systematic differences in metabolic potential that support these observations. We also observe higher levels of selective forces acting on habitat-specific metabolic genes linked to SAR11 fitness and polyphyletic distributions of habitat preferences and metabolic traits across SAR11 genera, suggesting that contrasting lifestyles have emerged across multiple lineages independently. Together, these insights reveal niche-partitioning within sympatric and parapatric populations of SAR11 and demonstrate that the immense genomic diversity of SAR11 bacteria naturally segregates into ecologically and genetically cohesive units, or ecotypes, that vary in spatial distributions in the tropical Pacific.

Main

Bacterial populations typically harbor extensive variation in gene content that can be difficult to delineate into discrete ecological or evolutionary units, despite the significant impact such differences may have on the biogeochemical roles, ecological interactions, and fitness of these microorganisms (Louca et al. 2016; Hao et al. 2020; Wang et al. 2023). Comparative genomics has enabled the identification of gene content variation that underpins distinct ecologies and contributes to the process of niche diversification (Cordero and Polz 2014; Sheppard et al. 2018; Whelan et al. 2021). However, because these analyses most often use a collection of genomes isolated from diverse environments where genes have evolved under a range of selective pressures (Conrad et al. 2022), associating variations in gene content with specific forces of selection and identifying crucial genes that likely serve as determinants of fitness under specific conditions remains a formidable challenge.

The bacterial order *Pelagibacterales* (SAR11) is one of the most abundant and diverse bacterial groups in the surface oceans (Morris et al. 2002; Brown et al. 2012; Grote et al. 2012), where even a single SAR11 population can exhibit substantial sequence diversity in the environment (Delmont et al. 2019). Defining the genomic variation underlying distinct spatial distributions of SAR11 populations and how gene content differs across environmental conditions is vital to further understanding ocean biogeochemical cycling, eco-evolutionary relationships, and the biology of a ubiquitous and dominant lineage in the surface oceans. This task remains difficult because assessing the loss or gain of ecologically-relevant genes or metabolic pathways in SAR11 necessitates a robust collection of high quality genome sequences that represent a spectrum of both ecological and genomic diversity. SAR11 cells are historically

recalcitrant to laboratory cultivation, and as such only a small portion of the total diversity of naturally occurring SAR11 populations can be interrogated via high quality genomes such as those from isolated strains (Haro-Moreno et al. 2020). Yet even with a small set of isolate genomes, SAR11 has become a key model to help elucidate fundamental processes of ecology and evolution such as genome streamlining (Giovannoni et al. 2005), marine oligotrophy (Noell et al. 2023), co-evolution (Morris et al. 2012; Braakman et al. 2017), drivers of genetic diversity and evolution within organisms of large population sizes (Vergin et al. 2007; Delmont et al. 2019), structure-aware investigations of microbial population genetics (Kiefl et al. 2023), and ocean biogeochemical cycling (Grant et al. 2019; White et al. 2019; Acker et al. 2022).

In our companion work (Freel et al. 2024), we address the gap in the available genomic resources with novel SAR11 isolates that originate from a geographically constrained environment within the tropical Pacific, and develop a phylogenomic backbone that unites evolution with ecology to understand this diverse clade. Freel et al., (2024) delineated four families within SAR11, including the family *Pelagibacteraceae* which encompasses the historical SAR11 subgroups Ia and Ib. Here, we illuminate metabolic diversity found within *Pelagibacteraceae* and identify the determinants of niche differentiation within co-occurring *Pelagibacteraceae* populations by combining 71 of the new isolates with 21 previously sequenced *Pelagibacteraceae* isolate genomes. By taking advantage of metagenomes from the prominent source of isolation, we apply an integrated ‘omics analysis to unveil differences in *Pelagibacteraceae* metabolic features across coastal and offshore habitats and identify metabolic genes under high selective pressures.

Results

Ecology and evolution of *Pelagibacteraceae* reveals strong habitat-specificity

By analyzing 92 high quality genomes from isolates obtained predominantly from coastal Kāneʻohe Bay, Oʻahu, Hawaiʻi, and the adjacent offshore (**Fig. 1, Supplementary file 1a**), we reveal that the genomic diversity of cultured *Pelagibacteraceae* partitions into eleven discrete monophyletic clusters, seven of which include isolates from the Kāneʻohe Bay Time-series (KByT; **Fig. 1, Extended Data Fig. 1a**). The 92 genomes belong to both previously-described and new clades, which we recently described as eleven genera (Freel et al. 2024; **Fig. 1**, **Supplementary file 1a**). The within-genus genome-wide average nucleotide identity (gANI) differed among genera, with the lowest within-genus average gANI found in *Proprepelagibacter* (87.1±0.0%, mean ± sd) and the highest within-genus average gANI found in *Littoralipelagibacter* (95.8±0.0; **Supplementary file 1b**). The average of all within-genus genome-wide average nucleotide identities was 92.3±2.7%.

We investigated the biogeography of *Pelagibacteraceae* isolate genomes through read recruitment with metagenomes from KByT and Station ALOHA in the adjacent North Pacific Subtropical Gyre. This revealed that the seven genera within the *Pelagibacteraceae* that contained KByT isolate genomes were commonly detected within the KByT system, while the three genera not containing KByT isolates were rarely detected, if at all (**Extended Data Fig. 1b**). Congruent with k-means cluster analysis that grouped the biogeochemical parameters from the metagenomic samples into coastal and offshore clusters (**Extended Data Fig. 3,**

105 **Supplementary file 1c, Supplementary Information Note 1**), the patterns of genome
106 distribution revealed a clear dichotomy where each genus was either highly present in the
107 offshore or in the coastal environment, but not both (**Fig. 1c, Supplementary file 1d**). Genera
108 with higher abundances in the coastal environment, hereafter referred to as 'coastal genera', did
109 not occur within a single monophyletic clade and instead appeared to have evolved multiple
110 times across the evolutionary history of *Pelagibacteraceae* (**Fig. 1c**).

111 For the most part, the patterns of distribution were consistent for all genomes within the
112 same genus (**Extended Data Fig. 3**), and genomes that belonged to the same genus generally
113 recruited similar proportions of reads from the environment. One exception was the genome
114 HIMB1412 from the genus *Coralipelagibacter* which had the highest relative abundance among
115 all *Pelagibacteraceae* genomes in the coastal environment (19.9±9.4%, mean ± sd, **Extended**
116 **Data Fig. 3**). While we consistently detected all isolate genomes of *Xanthipelagibacter* in the
117 offshore environment, three of eight genomes (HIMB83, FZCC0015, HIMB1456) were also
118 frequently detected in the coastal environment (**Extended Data Fig. 3**). Regardless, their relative
119 abundances were low in coastal samples (0.4±0.5%, mean ± sd) and sharply increased offshore
120 (3.5±2.0%, mean ± sd; **Extended Data Fig. 3**), further supporting the characterization of
121 *Xanthipelagibacter* as an offshore genus.

122 Overall, our metagenomic read recruitment reveals that *Pelagibacteraceae* communities
123 partition between coastal and offshore habitats in the tropical Pacific, that these distinct
124 communities are driven by differences in the distribution of individual *Pelagibacteraceae*
125 genera, and that coastal genera (*Ampluspelagibacter*, *Coralipelagibacter*, *Littoralipelagibacter*)
126 are distributed polyphyletically across the *Pelagibacteraceae*.

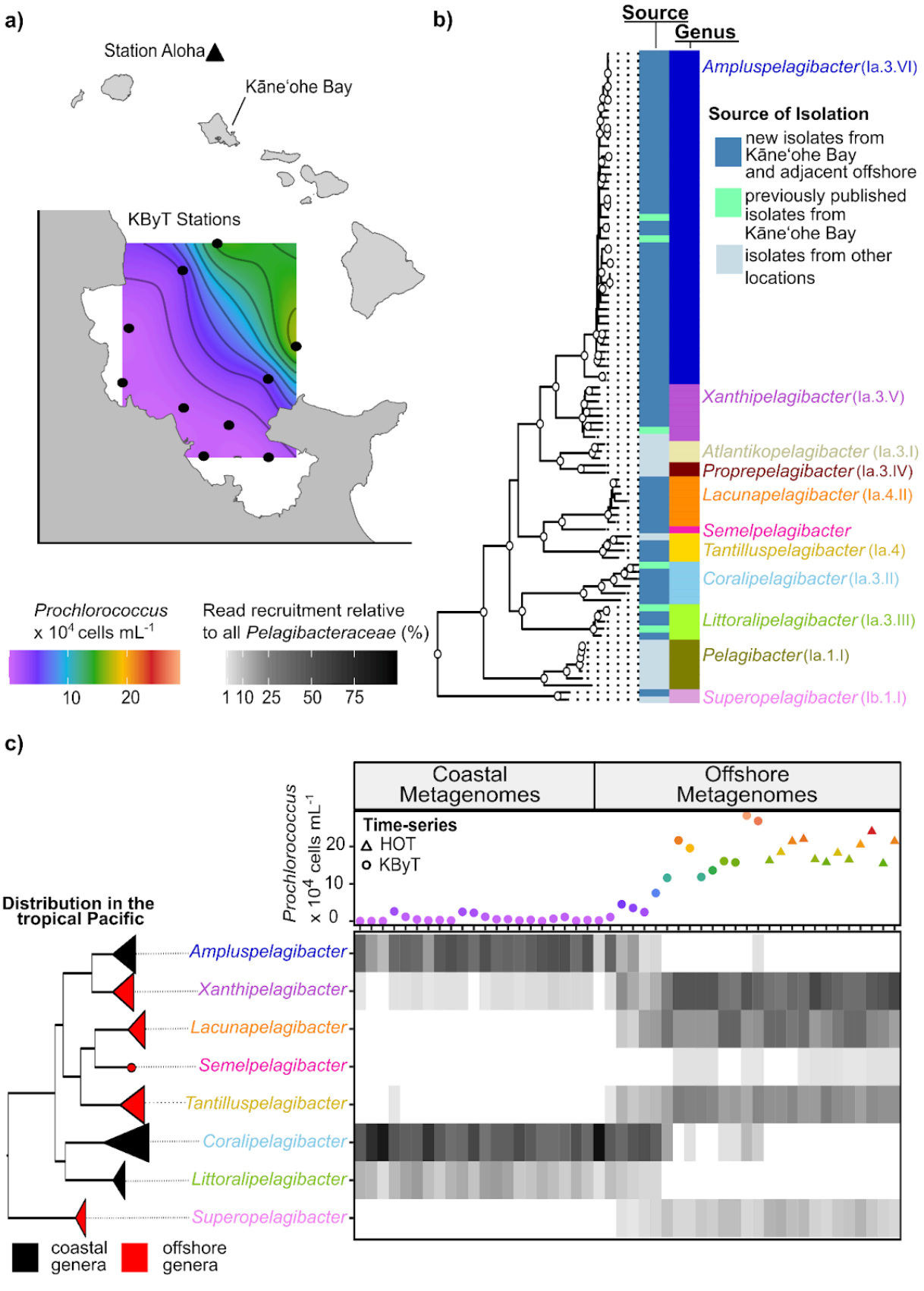
a)
Station Aloha
Kāneʻohe Bay
KByT Stations
Prochlorococcus
x 10^4 cells mL^-1
10
20
Read recruitment relative
to all Pelagibacteraceae (%)
1 10 25 50 75
b)
Source
Genus
Ampluspelagibacter (Ia.3.VI)
Source of Isolation
new isolates from Kāneʻohe Bay and adjacent offshore
previously published isolates from Kāneʻohe Bay
isolates from other locations
Xanthipelagibacter (Ia.3.V)
Atlantikopelagibacter (Ia.3.I)
Proprepelagibacter (Ia.3.IV)
Lacunapelagibacter (Ia.4.II)
Semelpelagibacter
Tantilluspelagibacter (Ia.4)
Coralipelagibacter (Ia.3.II)
Littoralipelagibacter (Ia.3.III)
Pelagibacter (Ia.1.I)
Superopelagibacter (Ib.1.I)
c)
Coastal Metagenomes
Offshore Metagenomes
Prochlorococcus
x 10^4 cells mL^-1
20
10
0
Time-series
HOT
KByT
Distribution in the tropical Pacific
Ampluspelagibacter
Xanthipelagibacter
Lacunapelagibacter
Semelpelagibacter
Tantilluspelagibacter
Coralipelagibacter
Littoralipelagibacter
Superopelagibacter
coastal genera
offshore genera

127

Fig. 1. ***Pelagibacteraceae* show polyphyletic habitat preferences for coastal or offshore environments across KByT. a**) The location of the Kāneʻohe Bay Time-series (KByT) sampling stations and the Hawaii Ocean Time-series at Station ALOHA. KByT spans a steep biogeochemical gradient, as noted by the dramatic increase in *Prochlorococcus* cellular abundances immediately offshore. **b**) Eleven genera are represented by genome-sequenced *Pelagibacteraceae* isolates, with the majority isolated from coastal Kāneʻohe Bay and the adjacent offshore. Nodes with circles represent ≥90% bootstrap support. Historically referenced clade names for *Pelagibacteraceae* genera are provided in parentheses. **c**) The relative read recruitment of *Pelagibacteraceae* isolate genomes summed at the level of genera for metagenomes from KByT and Station ALOHA. Metagenomes grouped into two clusters by environmental parameters, coastal and offshore, coinciding with the gradient in *Prochlorococcus* cellular abundances. *Pelagibacteraceae* genera showed distinct distribution patterns in the coastal and offshore waters that are distributed polyphyletically. Read recruitment <1% not shown.

Pelagibacteraceae pangenome includes differentially enriched genes and functions within coastal and offshore genera

Next, we sought to characterize the genomic diversity and functional gene content of *Pelagibacteraceae* isolates in order to investigate the potential determinants of fitness that may explain the distinct ecological patterns of distribution. We utilized a pangenomic approach that partitioned all genes across all *Pelagibacteraceae* genomes into *de novo* gene families, or ‘gene clusters’, based on amino acid sequence homology. This analysis resulted in 8,242 gene clusters across all 92 genomes, of which 784 were core among all *Pelagibacteraceae* and made up the majority (52-63%) of gene content found in any individual genome (**Fig. 2a; Supplementary file 2a**). Half of the pangenome was composed of gene clusters that were singletons (4,201 of 8,242; **Fig. 2a**). Between the extremes of gene clusters that occur in every genome and those that occur only in one, we found 206 accessory gene clusters that were ‘genus-specific’ (21±27, mean±sd per genus; **Fig. 2a**; **Supplementary file 2b**) as they were present among all representatives of a single genus, but absent from genomes belonging to any other genus. The 206 genus-specific gene clusters were not distributed uniformly across genera, as 95 were unique

159 to the genus *Superopelagibacter* alone (**Supplementary file 2b**). However, this number is likely
160 an overestimation of the true *Superopelagibacter* genus-specific traits since this particular genus
161 was represented by only two genomes, and the number of genus-specific gene-clusters
162 negatively correlated with the number of genomes in a genus (r^2adj = 0.37, F=6.29, p = 0.037;
163 Pearson's correlation). Gene clusters that were core to multiple genera (e.g., present in every
164 genome for two or more genera, but absent in every other) were also not a dominant feature in
165 the pangenome (**Fig. 2a**). They only represented 182 gene clusters, and were generally uniformly
166 distributed across many different groupings of genera (**Fig. 2a**; **Supplementary file 2b**). We
167 could further assign a subset of the gene clusters to coastal or offshore categories based on the
168 environmental preference of the genomes in which they occurred, finding 32 and 125 gene
169 clusters that were specific to coastal genera and offshore genera, respectively. (**Fig. 2a,**
170 **Supplementary file 2b**).

171 We next focused on genes with well-characterized roles in known metabolisms by
172 examining those that share orthology with genes described in the Kyoto Encyclopedia of Genes
173 and Genomes (KEGG; Kanehisa and Goto 2000) through KOfam models (Aramaki et al. 2020)
174 and generating a 'functional pangenome' (**Fig. 2b**). The *Pelagibacteraceae* functional
175 pangenome grouped genes based on functional identity rather than amino acid sequence
176 similarity and consisted of 1,276 KOfam functions, with a large core (612 KOfams; **Fig. 2b**).
177 Many of the remaining non-core functions were still shared widely across all eleven genera with
178 a relatively uniform distribution (n=136; **Fig. 2b**) or were singletons (n=70). Similar to the
179 conventional pangenome, the functional pangenome contained very few genus-specific functions
180 (14 total among all genera; 0-5 KOfams per genus; **Fig. 2b**) and a limited number of functions
181 that were core to multiple genera (e.g. present in every genome for two or more genera, but

182 absent in every other; 32 KOfams total; **Fig. 2b; Supplementary file 2c**). Only three KOfam
183 functions were specific to coastal genera, while 13 KOfam functions were specific to offshore
184 genera (**Fig. 2a; Supplementary file 2c**).

185 Pangenomic analysis using conventional and functional approaches revealed a large
186 overlap in gene content among ecologically distinct genera, with subtle but consistent
187 genus-specific features. The high overlap in gene content across the *Pelagibacteraceae* and small
188 number genus-specific gene clusters suggests differentiation between genera of the
189 *Pelagibacteraceae* may be determined by only a small portion of the genome. The polyphyletic
190 distribution of habitat preference (**Fig. 1c**) supports that genes and functions that are linked to
191 success in these different habitats likely evolved multiple times through independent processes.
192 Given this evolutionary trajectory, it is highly plausible that instead of vertical inheritance,
193 horizontal gene transfer led to the acquisition of most of these habitat-specific genes and
194 subsequent high rates of recombination and strong selective forces resulted in the increased
195 prevalence among *Pelagibacteraceae* in a given ecological niche. This process, referred to as
196 gene-specific sweeps, frequently results in a more subtle display of habitat-specific traits
197 (Shapiro et al. 2016), as is observed here. To further examine the potential importance of these
198 environmentally-distinct functions in providing advantages to *Pelagibacteraceae* prevalent in
199 coastal or offshore habitats, we next focused on the subset of the environmentally-distinct
200 functions characterized here that are involved in nutrient resource utilization and cellular stress.
201 Furthermore, in examining the functions involved in nutrient resource utilization and cellular
202 stress, we broadened our investigation beyond the functions that were strictly found in coastal
203 genera or strictly found in offshore genera (e.g. environmentally-distinct functions), to also
204 include functions that were enriched in either coastal or offshore genera.

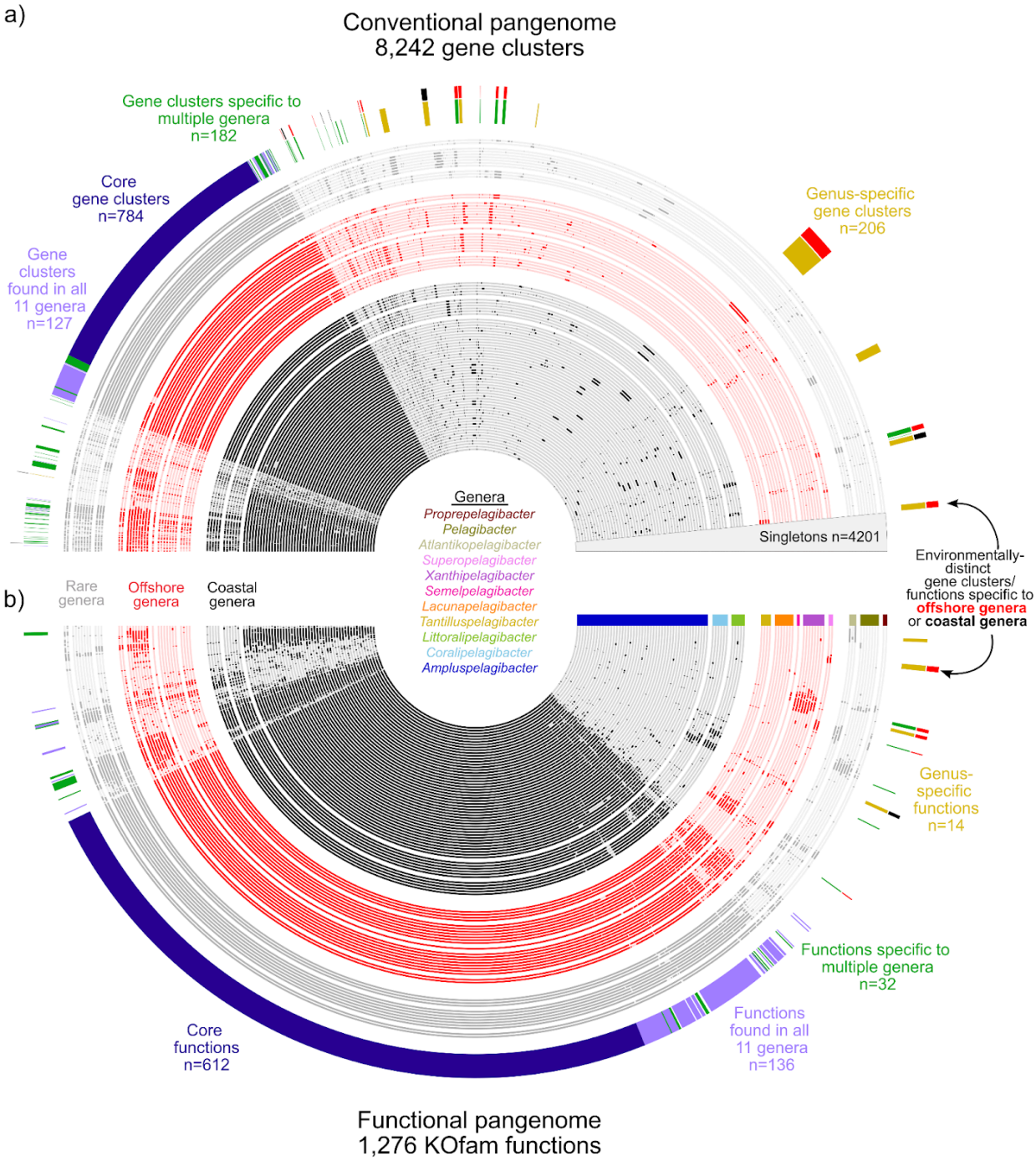

Fig 2. *Pelagibacteraceae* genomes share high overlap in genes and functions among ecologically-distinct groups. The presence and absence of gene clusters and KOfams are shown across **a)** a conventional pangenome and **b)** a functional pagenome, respectively. Genomes (inner rings) are grouped by genus and further grouped by ecological distribution in the tropical Pacific as coastal, offshore, or rare. The distribution of the gene pool and functions in the second most outer layer (e.g., core, genus-specific) show that the gene pool and functions are shared

extensively across all 11 genera and 92 genomes. The outer layer shows the sparse environmentally-distinct portions of the gene pool and functional pool that are specific to coastal or offshore genera.

Potential determinants of habitat-specificity in *Pelagibacteraceae* include molybdenum utilization and nitrogen and carbon metabolisms

Despite a high amount of water exchange, coastal Kāneʻohe Bay and the adjacent offshore vary in nutrient availability, osmotic conditions (e.g. salinity, temperature, pH), and phytoplankton communities that determine the organic carbon pool (Tucker et al. 2021, 2024), suggesting that this would enforce distinct environmental pressures on coastal and offshore *Pelagibacteraceae* genera. To characterize ecologically-relevant genes that may support coastal and offshore habitat-preferences of *Pelagibacteraceae* across the KByT system, we used an enrichment analysis to examine metabolic traits related to nutrient acquisition and cellular stress that were differentially distributed across genomes from either coastal or offshore genera. Genes that were core across genera of the *Pelagibacteraceae* or did not show easily distinguishable distributions (e.g. driven by phylogeny or environment) are further discussed in **Supplementary Information Note 2**. Unless noted otherwise, the following metabolic traits were found outside of hyper-variable regions of genomes and thus represent genes that are encoded within the relatively stable genomic backbones of a given genus or set of genera.

Molybdenum enzyme utilization.

Molybdenum enzymes are nearly ubiquitous among organisms from all domains of life, catalyze important oxidation-reduction reactions involved in carbon, sulfur, and nitrogen

235 metabolisms, and require a cofactor scaffold to hold the molybdenum in place (Zhang and
236 Gladyshev 2008). While most *Pelagibacteraceae* genomes contained genes involved in
237 molybdenum cofactor biosynthesis as well as molybdenum cofactor-dependent enzymes (**Fig.**
238 **3a, Supplementary file 2d**), these genes were missing from two offshore genera,
239 *Lacunapelagibacter* and *Tantilluspelagibacter*. In contrast to the lack of molybdenum enzymes
240 found in the offshore *Lacunapelagibacter* and *Tantilluspelagibacter*, other offshore genera,
241 *Xanthipelagibacter* and *Semelpelagibacter*, appeared to increase reliance on
242 molybdenum-dependent enzymes by uniquely harboring genes encoding
243 molybdenum-dependent enzymes associated with the oxidation of purines (xanthine; *xdhAB*)
244 (**Fig. 3a, Supplementary file 2d, Supplementary Note 3**). The distribution of molybdenum
245 enzymes are polyphyletically distributed among offshore genera, where some offshore groups
246 possess no molybdenum enzymes while others harbor all the molybdenum enzymes detected
247 within *Pelagibacteraceae* (**Fig. 3a**). We hypothesize that the absence of molybdenum enzymes
248 within the offshore *Lacunapelagibacter* and *Tantilluspelagibacter*, which have some of the
249 smallest genomes within *Pelagibacteraceae* (~1.2Mbp; **Supplemental file 1a**), is likely driven
250 by streamlining selection to minimize metabolic requirements and genome size (Giovannoni et
251 al. 2005, 2014).

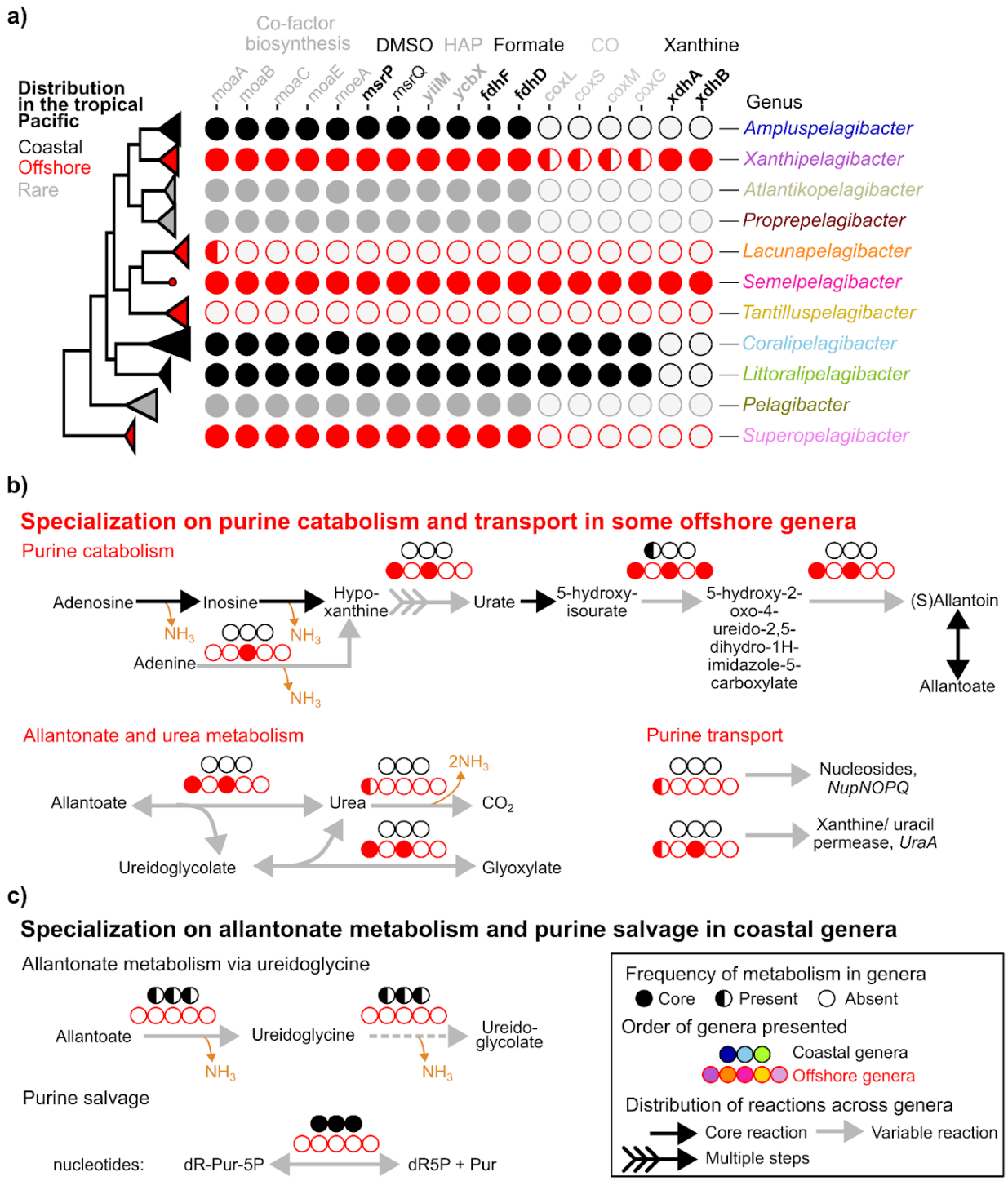

Fig. 3. *Pelagibacteraceae* genera fill distinct niches in molybdenum enzyme utilization. a) The distribution of molybdenum cofactor (MoCo) biosynthesis genes and genes involved in metabolisms that require a molybdenum cofactor across *Pelagibacteraceae* genera. Metabolisms within *Pelagibacteraceae* that require a molybdenum cofactor included those involved in the repair of methionine sulfoxides and the catalytic subunit of periplasmic dimethylsulfoxide

(DMSO; *msrPQ*), the detoxification of 6-N-hydroxylaminopurine (HAP) to adenine (*yiiM*, *ycbX*), the oxidation of formate to carbon dioxide (*fdhFD*), the oxidation of carbon monoxide (*coxSMLG*), and the oxidation of purines (*xdhAB*). Genes that are predicted to represent proteins with molybdenum cofactor binding sites are noted in bold. **b)** Genes encoding for purine catabolism and transport are only present in some offshore genera**. c)** Genes encoding for allantonate metabolism and purine salvage are present only in coastal genera. MoCo: molybdenum cofactor, DMSO: dimethylsulfoxide, HAP: hydroxylaminopurine, CO: carbon monoxide, NH_3: ammonia, dR-Pur-5P: purine 2'-deoxyribonucleoside 5'-monophosphate, Pur: purine base, dRib5P: 2'-deoxyribonucleoside 5'-monophosphate, (d)R-Pur-1P: beta-(deoxy)ribonucleosides.

Nitrogen metabolisms.

Purines are abundant in aquatic environments (Berman and Bronk 2003), contain a high number of nitrogen atoms per molecule (Kornberg 1974), and likely contribute to niche-differentiation between coastal and offshore SAR11 (Braakman et al. 2024). Our metabolic reconstructions show that offshore genera *Xanthipelagibacter* and *Semelpelagibacter* harbored genes to catabolize purines through the utilization of a molybdenum cofactor-dependent xanthine dehydrogenase (**Fig. 3b, Supplementary file 2e**), as well as genes with functions predicted to support the efficient transport of nucleotides (*Xanthipelagibacter*: *nupNOPQ* system; *Xanthipelagibacter* and *Semelpelagibacter*: xanthine/uracil permease *uraA*). To make hypoxanthine available for degradation, *Semelpelagibacter* can convert adenine to hypoxanthine using adenine deaminase (*ade*) and both genera *Semelpelagibacter* and *Xanthipelagibacter* also uniquely possess a tRNA(adenine34) deaminase (*tadA*), which can convert adenine to hypoxanthine (**Fig. 3b**). Most *Xanthipelagibacter* genomes (6 of 8) also harbor a urease system (*ureABCDEFG*) to liberate ammonia in the final steps of the xanthine degradation pathway.

In contrast to the purine degradation pathways found within the offshore genera, we found coastal genera specialize on the degradation of allatonate, a bi-product of purine metabolism, as well as the recycling of nucleotides. Members of the coastal genus

286 *Ampluspelagibacter* (and a single *Coralipelagibacter* genome, HIMB5) have the functional
287 capacity to degrade allantoate to (S)-ureiodoglycine and ammonia via an allantoate deiminase
288 and ureidoglycine to ureidoglycolate and ammonia, via a nucleophile (Ntn)-hydrolase (**Fig. 3c,**
289 **Supplementary file 2e**). It is important to note that the allantoin degradation genes found in
290 coastal genomes characterized here appear to provide a source of nitrogen, and differ from those
291 found in the offshore genera. All coastal genera possess a deoxynucleoside 5-monophosphate
292 N-glycosidase (*rcl*) that putatively breaks the N-glycosidic bond of purine nucleotides (i.e.
293 purine 2'-deoxyribonucleoside 5'-monophosphates; **Fig. 3c**). This differs from the purine
294 nucleoside salvage pathway core to both coastal and offshore genera, which requires
295 orthophosphate to cleave the N-glycosidic bond of beta-(deoxy)ribonucleosides to yield
296 alpha-(deoxy)ribose 1-phosphate (**Supplementary file 2e**). All *Pelagibacteraceae* are missing
297 genes to utilize deoxyribose-5-phosphate or deoxyribose-1-phosphate via a
298 deoxyribose-phosphate aldolase (*deoC*). However, ribose-1-phosphate could be catabolized to
299 D-fructose-6P and D-glyceraldehyde-3P (**Supplementary file 2e**).
300 In addition to differences in purine metabolism, offshore genera uniquely harbor a
301 transaminase (*agxt*) that may help these cells to overcome an auxotrophy for the biosynthesis of
302 the amino acid glycine (**Fig. 4, Supplementary file 2f**), which is a common feature across
303 *Pelagibacteraceae*, but likely restricts important biosynthetic pathways including protein
304 synthesis and central carbon metabolism (Tripp et al. 2009). Offshore genera also uniquely
305 contain genes involved in glutamate deamination, glutathione and carnitine metabolism, and the
306 synthesis of glucosylglycerate, which is used as an alternative osmolyte under nitrogen-limited
307 conditions in cyanobacteria (Klähn et al. 2010). In contrast, the coastal genera contain nitrogen
308 metabolisms generally involved in the deamination of various amino acids (e.g. hydroxyprolines,

309 proline, ornithine, and threonine). A subset of coastal *Ampluspelagibacter* genomes also have the
310 potential to metabolize the polyamines putrescine and spermidine via *puuBCD* (**Fig. 4**). The
311 puuD gene was located in hypervariable regions within coastal *Ampluspelagibacter* genomes.

312 Phosphate & Metals.

313 Some offshore *Pelagibacteraceae* genera exhibit a reduced genomic capacity to transport
314 phosphate relative to coastal genera. High-affinity phosphate acquisition genes (*pstSCAB-phoU*;
315 *phoB*; *phoR*) were core among coastal genera but, while present in some genomes, were not core
316 among the offshore genera. Offshore genomes lacking this system appear to rely solely on the
317 *pitA* gene, a presumably lower-affinity proton-motive force permease of phosphate or sulfur
318 (**Fig. 4, Supplementary file 2f**). Some offshore genera contain an increased genomic capacity to
319 transport or capture iron relative to coastal genera. While all *Pelagibacteraceae* contain an iron
320 (III) transport system (*afuAB*), the offshore *Semelpelagibacter* genus alone possesses a
321 high-affinity iron permease (*ftr1*) (**Fig. 4, Supplementary file 2f)**. Offshore genera
322 *Superopelagibacter*, *Lacunapelagibacter*, and *Tantilluspelagibacter* also contain a heme oxidase,
323 which could catalyze the oxidative degradation of the heme porphyrin ring to release iron.
324 Unique genes to utilize copper, potassium, and nickel were found among the coastal genera (**Fig.
325 4)**. We observed a copper-containing plastocyanin gene within a small subset of coastal genomes
326 (**Fig. 4; Supplementary file 2f**). Plastocyanins serve as an electron carrier from cytochrome *f* to
327 photosystem I and are generally found within eukaryotic phytoplankton and cyanobacteria
328 (Castell et al. 2021). Future studies are needed to understand the functional role of plastocyanins
329 in *Pelagibacteraceae*, although one potential use could be the storage of copper to cope with
330 periods of reduced availability (Peers and Price 2006).

Cellular stress.

Differences in the capacities to respond to osmotic and oxidative stresses were found among offshore and coastal *Pelagibacteraceae* genera. Most offshore genera shared a catalase-peroxidase (*katG*) that may help to cope with oxidative stress and has also been suggested to play a role in the co-evolution of marine microbial communities (Morris et al. 2012) (**Fig. 4, Supplementary file 2f**). Coastal genera contained two genes involved in osmotic stress that were not prevalent among offshore genomes: a voltage-gated sodium channel (*vgsc*) and a cation:H+antiporter (*yrbG*) (**Fig. 4, Supplementary file 2f**). Voltage-gated sodium channels utilize a structurally complex gating system to physically open and close the pore in response to changes in fluid shear or membrane stretch from dehydration (Ren et al. 2001; Strege et al. 2023), and may be particularly useful in coastal Kāneʻohe Bay where spatiotemporal shifts in salinity are common (Yeo et al. 2013).

Carbon metabolisms.

Carbon metabolisms unique to coastal and offshore genera were remarkably distinct. SAR11's specialization on low-molecular weight, labile carbon sources has likely facilitated the success of this marine oligotroph in open oceans where carbon substrates are limited in availability and under high competition (Sun et al. 2011; Giovannoni 2017; Moore et al. 2022). Consistent with these observations, the carbon metabolisms shared by offshore genera did not rely on glycolysis and involved low-molecular-weight compounds (one-carbon to three-carbon; C1-C3) that are common molecules and/or typical waste products in the marine environment. This includes the genetic potential to metabolize organic acids such as D-lactate, oxalate, haloacetate, and formate, as well as diverse aldehydes (**Fig. 4**, **Supplementary file 2f**). In

353 contrast, coastal genera contain gene content to specialize in the degradation of relatively larger
354 carbon compounds (C4-C6), including the sugars D-xylulose and D-ribulose via *xylB* and sugar
355 alcohols arabinitol and mannitol via an arabinitol dehydrogenase, both of which subsequently
356 enter glycolysis through the non-phosphorylative Entner–Doudoroff (np-ED) pathway. Some
357 coastal groups also have the capacity to metabolize the sugar acids D-tartrate and malate via
358 *tarD* (**Fig. 4; Supplementary file 2f**). Genomes belonging to the coastal genus
359 *Ampluspelagibacter*, which have the largest genomes among known *Pelagibacteraceae*,
360 harbored gene content potentially involved in the transport and metabolism of
361 glycerophospholipids and sn-glycerol-3-phosphate (*glpA*, *upgEBQ*, *gpr*), the capacity to
362 metabolize L-fucose, D-arabinose, and L-xylose to pyruvate through a L-fucono-1,5-lactonase
363 (*fucB*) and the glycolytic Entner-Doudoroff (ED) glycolytic pathway, and a fructose transport
364 system (*frcABC*) (**Fig.4; Supplementary file 2f**). The ED glycolytic pathway was core among
365 *Ampluspelagibacter*, *Xanthipelagibacter*, and *Proprepelagibacter* genomes and variable across
366 genomes in other genera (**Supplementary file 2f**). The increased prevalence of sugar
367 metabolisms among coastal genera, especially the *Ampluspelagibacter* genus, suggests
368 broadened metabolic versatility among coastal *Pelagibacteraceae* in response to a diverse and/or
369 more readily available set of organic carbons found within coastal Kāneʻohe Bay relative to
370 offshore waters. The distinct distributions of carbon metabolisms resolved here also suggests
371 fine-scale niche partitioning along the sugar-acid spectrum within *Pelagibacteraceae* (Gralka et
372 al. 2023).

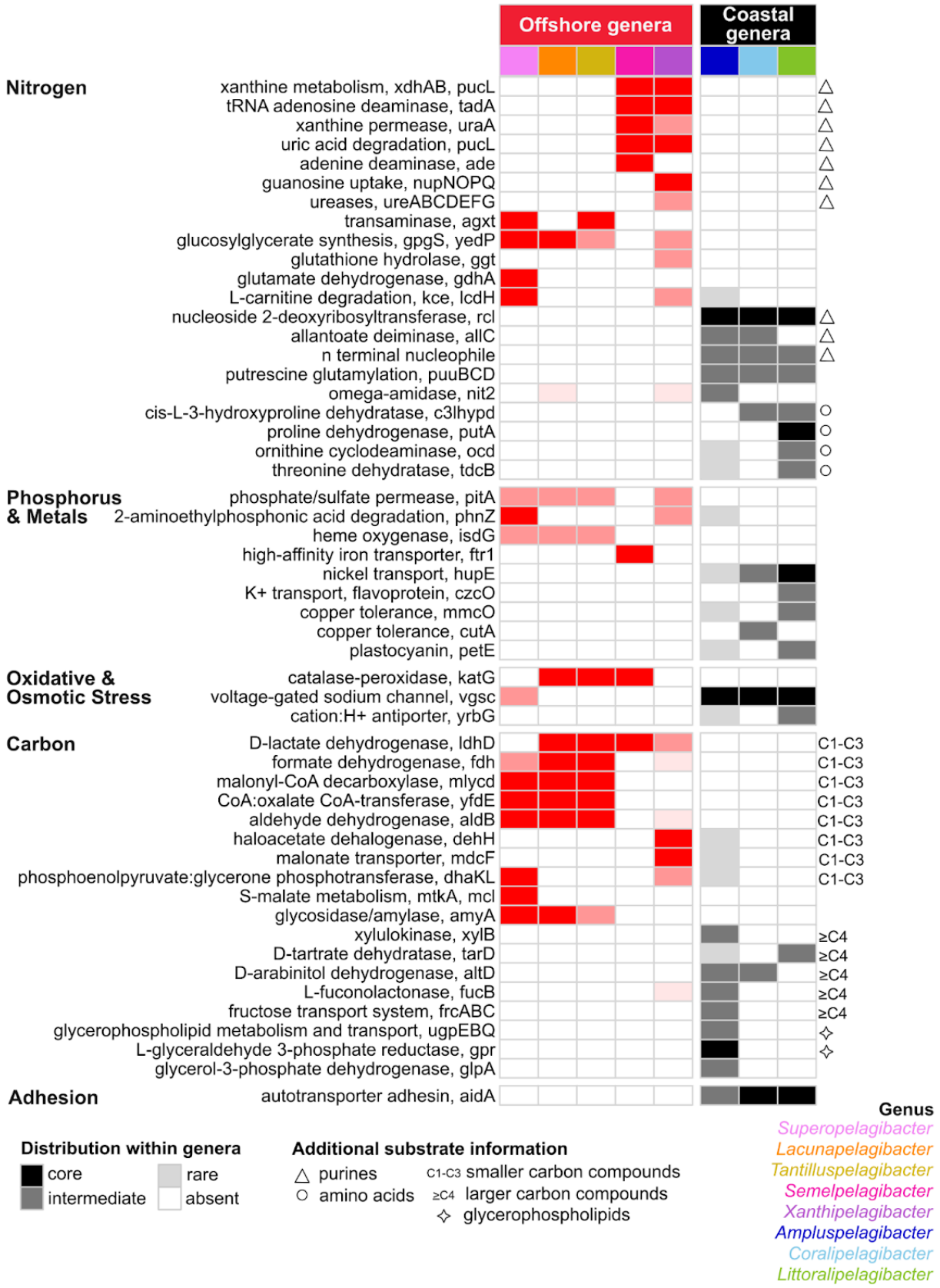
Offshore genera
Coastal genera
Nitrogen
xanthine metabolism, xdhAB, pucL
tRNA adenosine deaminase, tadA
xanthine permease, uraA
uric acid degradation, pucL
adenine deaminase, ade
guanosine uptake, nupNOPQ
ureases, ureABCDEFG
transaminase, agxt
glucosylglycerate synthesis, gpgS, yedP
glutathione hydrolase, ggt
glutamate dehydrogenase, gdhA
L-carnitine degradation, kce, lcdH
nucleoside 2-deoxyribosyltransferase, rcl
allantoate deiminase, allC
n terminal nucleophile
putrescine glutamylation, puuBCD
omega-amidase, nit2
cis-L-3-hydroxyproline dehydratase, c3lhypd
proline dehydrogenase, putA
ornithine cyclodeaminase, ocd
threonine dehydratase, tdcB
Phosphorus & Metals
phosphate/sulfate permease, pitA
2-aminoethylphosphonic acid degradation, phnZ
heme oxygenase, isdG
high-affinity iron transporter, ftr1
nickel transport, hupE
K+ transport, flavoprotein, czcO
copper tolerance, mmcO
copper tolerance, cutA
plastocyanin, petE
Oxidative & Osmotic Stress
catalase-peroxidase, katG
voltage-gated sodium channel, vgsc
cation:H+ antiporter, yrbG
Carbon
D-lactate dehydrogenase, ldhD
formate dehydrogenase, fdh
malonyl-CoA decarboxylase, mlycd
CoA:oxalate CoA-transferase, yfdE
aldehyde dehydrogenase, aldB
haloacetate dehalogenase, dehH
malonate transporter, mdcF
phosphoenolpyruvate:glycerone phosphotransferase, dhaKL
S-malate metabolism, mtkA, mcl
glycosidase/amylase, amyA
xylulokinase, xylB
D-tartrate dehydratase, tarD
D-arabinitol dehydrogenase, altD
L-fuconolactonase, fucB
fructose transport system, frcABC
glycerophospholipid metabolism and transport, ugpEBQ
L-glyceraldehyde 3-phosphate reductase, gpr
glycerol-3-phosphate dehydrogenase, glpA
Adhesion
autotransporter adhesin, aidA
C1-C3
≥C4
Distribution within genera
core
intermediate
rare
absent
Additional substrate information
purines
amino acids
C1-C3 smaller carbon compounds
≥C4 larger carbon compounds
glycerophospholipids
Genus
Superopelagibacter
Lacunapelagibacter
Tantilluspelagibacter
Semelpelagibacter
Xanthipelagibacter
Ampluspelagibacter
Coralipelagibacter
Littoralipelagibacter

373

Fig. 4. Metabolic determinants of habitat-specificity in *Pelagibacteraceae*. Metabolic genes associated with nutrient acquisition and cellular stress vary among coastal and offshore *Pelagibacteraceae* genera.

Adhesion.

Finally, while investigating the functional differences between coastal and offshore genera, we observed homologs of a large gene (~5,000 to 9,500 bp) annotated as an autotransporter adhesin that was almost always present among coastal genomes and absent in all offshore genomes (**Fig. 4**). Autotransporters provide a simple and relatively minimal mechanism for the delivery of a passenger protein to the surface of Gram-negative bacteria (Leyton et al. 2012), and can vary greatly in size due to changes in the number of repeating sequences in the passenger protein (Doyle et al. 2015). Because repeating regions cause difficulty for short-read assemblers such as those used in our genome assemblies (Freel et al. 2024), we further established confidence in the assembly of this gene in our coastal genomes by successfully finding homologs in long-read sequencing libraries from the coastal Kāneʻohe Bay environment and comparing protein structure models of genes annotated from the long-read data to a known autotransporter (**Extended Data Fig. 4; Supplementary Information Note 4**). We also examined the genome context of the gene, which was always positioned next to genes involved in type IV pilus systems and/or type II secretory systems and sometimes, but not always, within hyper-variable regions (**Extended Data Fig. 4, Supplementary Information Note 4, Supplementary file 2f**).

Adhesion to surfaces has not been observed in *Pelagibacteraceae* in culture or through environmental studies, although long filaments believed to be pili were observed within dividing cells of *Pelagibacteraceae* (Zhao et al. 2017) and are associated with multiple processes,

398 including adhesion to surfaces, transformation competence, and DNA uptake (Hazes and Frost
399 2008; Ellison et al. 2018). While speculative, it is possible that adhesion by the autotransporter
400 adhesin gene may be involved in the uptake of nutrients also in *Pelagibacteraceae* (Meuskens et
401 al. 2019). The coastal distribution of the autotransporter gene suggests that the advantage of
402 having this large of a gene is worth the trade-off of maintenance in more nutrient-rich coastal
403 environments, but potentially not in nutrient-limited offshore environments.

404 In summary, our investigation of the distribution of genes related to nutrient acquisition
405 and cellular stress that are unique to coastal and offshore genera reveals numerous subtle
406 differences in metabolic traits driven by the presence or absence of single genes (e.g. high
407 affinity iron transporters, voltage-gated sodium channel genes), but few differences in multi-gene
408 metabolic pathways (e.g. purine metabolism, molybdenum cofactor biosynthesis, fucose
409 metabolism). Differences in genes related to nutrient acquisition were predominantly related to
410 organic carbon and nitrogen metabolisms, and help to further define the unique and diverse roles
411 *Pelagibacteraceae* play in oceanic biogeochemical cycles. The distribution of these metabolic
412 traits generally do not follow phylogenetic distributions, but environmental patterns, suggesting
413 that these metabolisms may be driven by selective pressures from the environment.

414

415 Gene determinants of habitat-specificity are under relatively higher 416 selective pressures compared to non-diagnostic genes

417 Our analyses indicated a relatively small number of functions in the *Pelagibacteraceae*
418 appear to be associated with its strict niche partitioning. Assuming that the requirement to
419 perform optimally may be higher for genes that determine fitness to particular lifestyles, we
420 hypothesized that metabolic traits that have distinct environmental distributions should be under

421 higher selective pressures compared to other genes in the environment. To test this hypothesis we
422 examined the proportion of non-synonymous to synonymous (pN/pS) sites per gene across
423 *Pelagibacteraceae* genomes using four deeply sequenced metagenomic samples from the KByT
424 system.

425 To define the set of genomes to be included in this analysis, we first evaluated whether
426 the gene-level selective pressures were uniform across genomes from the same genus. We
427 examined variation in pN/pS across genes with shared KOfam assignments for genomes
428 belonging to the genus *Coralipelagibacter,* which has a low minimum gANI (84.5%, n=6) and is
429 abundant in the tropical Pacific. Gene-to-gene variation explained 82% of the variation, while
430 sample-to-sample variation and genome-to-genome variation only explained 0.26 and 0.09%,
431 respectively (ANOVA, **Supplemental file 3a**). The little genome-to-genome variation showed
432 that genomes within the same genus likely experience similar patterns of selection on shared
433 genes, and supported using a single genome as a representative per genus. Thus, our downstream
434 analyses utilized a single genome for each genus in *Pelagibacteraceae*, except
435 *Atlantikopelagibacter*, *Pelagibacter*, *Proprepelagibacter*, and *Semelpelagibacter*, which lacked
436 sufficient coverage in the KByT system (**Extended Data Fig. 1**, **Supplemental file 3b**).

437 Across the *Pelagibacteraceae* genomes examined, strong purifying selection (pN/pS $\ll$ 1)
438 was a general characteristic of most genes as observed previously by Kiefl et al., (2023), where
439 over 75% of genes in each genome representative had a pN/pS value of $\leq$ 0.1 (**Supplemental file**
440 **3c**). However, not all genes experienced similar magnitudes of purifying selection, with
441 gene-to-gene variation in pN/pS explaining between 88-99% of the variation in pN/pS across
442 genomes (n=7, ANOVA, **Supplemental file 3d**). Sample-to-sample variation in pN/pS values
443 varied for most genomes, however it explained a very small proportion of the overall variation

444 (<0.5%, n=7, ANOVA). Gene coverage showed no correlation between per gene values of pN/pS
445 (absolute value of r=0.02-0.28; Pearson correlation coefficient; **Extended Data Fig. 5**). Gene
446 coverage explained an extremely small portion of the overall pN/pS variation (<0.07%, n=7,
447 ANOVA, **Supplemental file 3d**), which indicates that pN/pS values are unlikely to be driven by
448 artifacts associated with variation in coverage.

449 We next evaluated the selective pressures on genes that were differentially distributed
450 across coastal and offshore *Pelagibacteraceae* genera (**Fig. 5; Extended Data Fig. 6)**. The
451 differentially distributed genes with the highest selective pressures in offshore genera included a
452 malonyl-CoA decarboxylase (*mlycd;* pN/pS= 0.019±0.010, mean ± sd), an aldehyde
453 dehydrogenase (*aldB*; pN/pS= 0.033±0.018), a formate dehydrogenase
454 (*fdh;*pN/pS=0.0127±0.001), a D-lactate dehydrogenase (*ldhD*; pN/pS=0.018±0.003) and an
455 alanine-glyoxylate / serine-glyoxylate / serine-pyruvate transaminase (*agxt*; pN/pS=
456 0.022±0.008) (**Fig. 5**). These genes are generally involved in the metabolism of small and
457 common carbon substrates and the capacity to produce glycine, which is an auxotrophy in other
458 *Pelagibacteraceae*. Within *Xanthipelagibacter*, genes involved in purine uptake (*uraA*,
459 pN/pS=0.040±0.001; *nupNOPQ*, pN/pS=0.045±0.010) experienced higher purifying selection
460 than purine degradation pathways (*xdhAB*, pN/pS=0.084±0.028), which is in line with previous
461 observations that high-affinity transport is key to *Pelagibacteraceae*'s success as an oligotroph
462 (Noell and Giovannoni 2019; Clifton et al. 2024). The low pN/pS values for these distinct carbon
463 and nitrogen related genes support the hypothesis that these metabolisms provide a fitness
464 advantage in offshore waters.

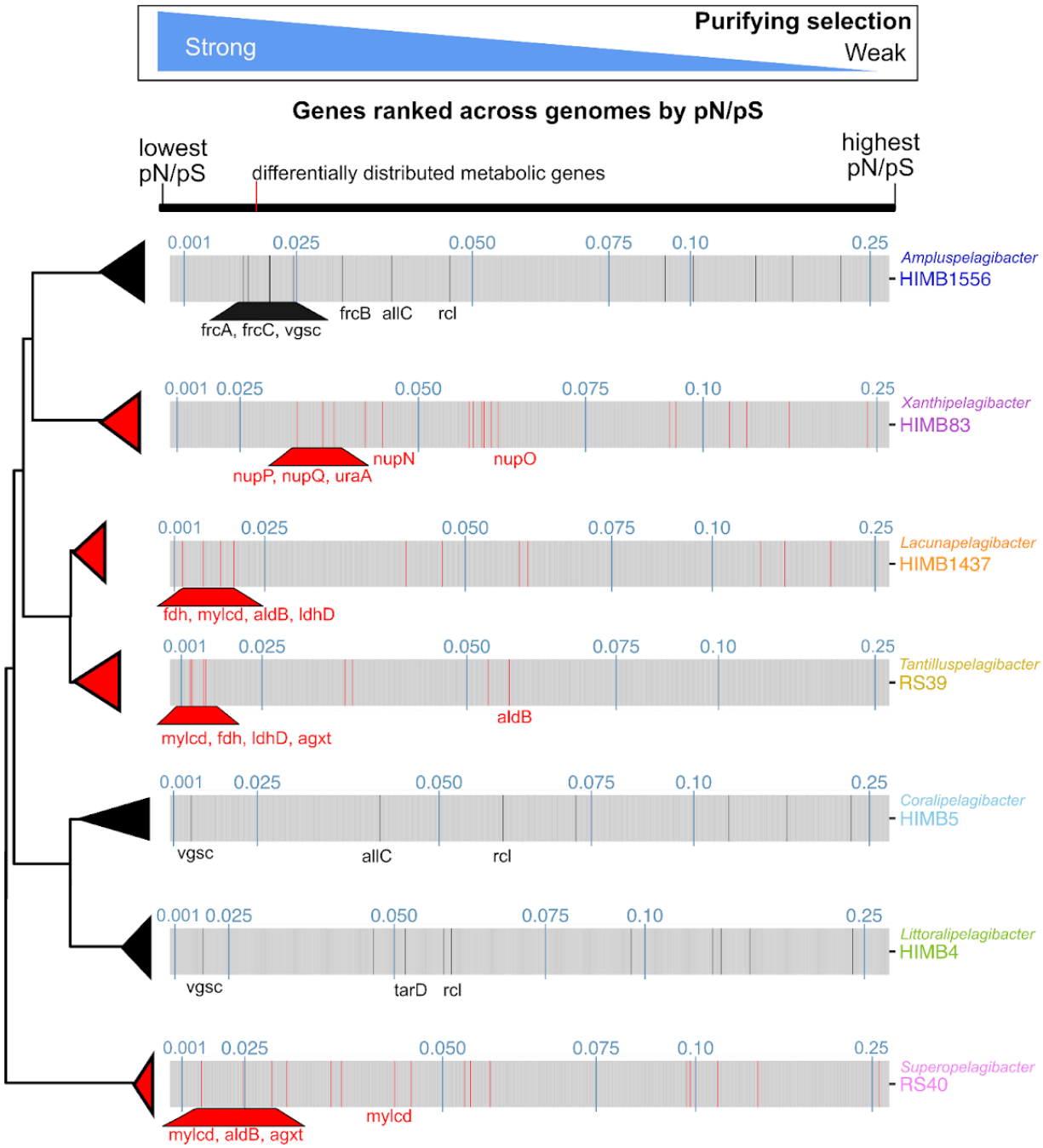

Ecologically-relevant genes for **offshore** and **coastal** genera

agxt	alanine-glyoxylate/ serine-glyoxylate/ serine-pyruvate transaminase	allC	allantoate deiminase
aldB	aldehyde dehydrogenase	frcABC	fructose transport system
fdh	formate dehydrogenase	rcl	nucleoside 2-deoxyribosyltransferase
ldhD	d-lactate dehydrogenase	tarD	d-tartrate dehydrogenase
mlycd	malonyl-CoA decarboxylase	vgsc	voltage-gated sodium channel
nupNOPQ	guanosine transporter		
uraA	xanthine permease		

466 **Fig. 5**. **Habitat-specific genes are under relatively higher selective pressures compared to**
467 **non-diagnostic genes.** pN/pS values per gene ranked from lowest to highest across each
468 genome. pN/pS values of 0.01, 0.025, 0.05, 0.075, 0.1, and 0.25 are shown in blue. Genes that
469 are differentially distributed between offshore and coastal *Pelagibacteraceae* genera in **Fig. 4** are
470 colored red (offshore) or black (coastal) across the genomes. For genes that are discussed in the
471 text, the gene names are noted and the description of the gene provided in the key. The full suite
472 of gene names and descriptions can be found in **Extended Data Fig. 6**.
473
474 Among the genes unique to coastal genera, the voltage-gated sodium channel was under
475 high selective pressure (*vgsc*, pN/pS=0.016±0.004). Coastal Kāneʻohe Bay harbors a larger range
476 of salinity, temperature, and pH conditions compared to the adjacent offshore (Yeo et al. 2013;
477 Tucker et al. 2021, 2024), and thus the voltage-gated sodium channels may be critical for coastal
478 genera as they rapidly regulate ionic composition (Ren et al. 2001). The allantoin deiminase
479 (*allC*, pN/pS=0.039±0.002) and nucleoside 2-deoxyribosyltransferase (*rcl*, pN/pS=0.054±0.006)
480 were also under moderately high selective pressures in coastal genomes, further supporting the
481 specialization of coastal genera on allantonate and nucleotides and a separation in purine
482 metabolism niche from offshore genera. Three sugar transporter genes (*frcABC*,
483 pN/pS=0.024±0.006) within *Ampluspelagibacter* and a tartrate dehydratase (*tarD*,
484 pN/pS=0.051±0.001) within *Littoralipelagibacter* exhibited low pN/pS values suggesting that
485 sugar metabolisms and transporters are not only a more common genomic feature in the coastal
486 genera, but also likely essential for their fitness.
487 Finally, to understand which *Pelagibacteraceae* core genes were under the highest
488 selective pressures in the KByT system, we examined the mean pN/pS values for core genes
489 found across the same seven genomes. Not surprisingly, ribosomal proteins were found among
490 the genes with the highest purifying selection (low pN/pS values; **Table 2**). Genes related to
491 baseline functions of the cell including general energy production and conversation, translational,
492 ribosomal structure and biogenesis, transcription, and nucleotide transport and metabolism were

493 also under high selective pressure (**Table 2**). Two genes involved in regulatory systems for
494 responses to acidity and glycine were among the top 25 core genes with the most purifying
495 selection. The low pN/pS values for these genes supports that although *Pelagibacteraceae* may
496 have few regulatory genes generally (Giovannoni et al. 2014), the ones it does have likely impact
497 the the performance and survival of *Pelagibacteraceae* cells.

498 Only two genes related to nutrient acquisition were found among the top 25 core genes
499 with the highest purifying selection. This included both subunits of the adenylylsulfate reductase
500 (*aprAB*), which is involved in dissimilatory sulfur metabolism, taking sulfite to adenylyl sulfate
501 (APS). Incomplete dissimilatory and assimilatory sulfate reduction pathways were core among
502 all *Pelagibacteraceae* examined in this study (**Extended Data Fig. 7**), in line with past analysis
503 of *Pelagibacteraceae* genomes (Tripp et al. 2008). As reported by Smith et al. (2016),
504 adenylylsulfate reductase likely removes sulfite that accumulates during organic sulfur
505 compound degradation. Further supporting this hypothesis, we found multiple core or near core
506 genes involved in the production of sulfite from reduced organosulfur compounds:
507 (2R)-sulfolactate sulfo-lyase (*suyAB*), a sulfoacetaldehyde acetyltransferase (*xsc*), and a sulfur
508 dioxygenase (**Extended Data Fig. 7**). Our analyses reveal the genetic potential to metabolize a
509 wide diversity of reduced organosulfur compounds as alternative sources of sulfur and that
510 adenylylsulfate reductases (*aprAB*) likely plays an important role in accommodating
511 *Pelagibacteraceae*'s unique sulfur metabolisms.

512

513

514

515

Table 2. **Core *Pelagibacteraceae* genes under high selective pressures in the KByT system**. The lowest 25 mean pN/pS values for core *Pelagibacteraceae* genes with shared KOfam annotations examined from genomes representing the seven *Pelagibacteraceae* genera that are highly abundant in the tropical Pacific. pN/pS: proportion of non-synonymous to synonymous. Enzymes involved in regulatory processes are denoted by a pound sign (#).

Accession	Description	pN/pS (mean±s.d.)
K02946	small subunit ribosomal protein S10	0.012±0.004
K00340	NADH-quinone oxidoreductase subunit K	0.013±0.008
K03560	biopolymer transport protein TolR	0.014±0.007
K03628	transcription termination factor Rho	0.014±0.004
K02078	acyl carrier protein	0.014±0.007
K03544	ATP-dependent Clp protease, subunit ClpX	0.017±0.004
K00053	ketol-acid reductoisomerase	0.017±0.005
K00395	adenylylsulfate reductase, subunit B	0.018±0.008
K00394	adenylylsulfate reductase, subunit A	0.018±0.005
K00412	ubiquinol-cytochrome c reductase cytochrome b subunit	0.018±0.006
K02274	cytochrome c oxidase subunit I	0.018±0.005
K02982	small subunit ribosomal protein S3	0.019±0.007
K03566#	LysR family transcriptional regulator, glycine cleavage system transcriptional activator	0.019±0.011
K01494	dCTP deaminase	0.019±0.006
K02878	large subunit ribosomal protein L16	0.019±0.008
K03798	cell division protease FtsH	0.019±0.005
K03702	excinuclease ABC subunit B	0.020±0.008
K00330	NADH-quinone oxidoreductase subunit A	0.020±0.010
K03569	rod shape-determining protein MreB	0.020±0.011
K02874	large subunit ribosomal protein L14	0.020±0.011
K14981#	two-component system, OmpR family, response regulator ChvI	0.020±0.01
K02988	small subunit ribosomal protein S5	0.021±0.005
K03046	DNA-directed RNA polymerase subunit beta	0.021±0.003
K03701	excinuclease ABC subunit A	0.021±0.003
K00331	NADH-quinone oxidoreductase subunit B	0.021±0.006

Discussion

Through genomic and metagenomic characterizations of a recently expanded collection of SAR11 isolates (Freel et al. 2024), our study reveals a polyphyletic distribution of coastal ocean versus offshore habitat specialists among closely related SAR11 populations, where the emergence of key genetic features that underlie this strong habitat preferences seem to have occurred through independent evolutionary events rather than transfer from a single common ancestor. Genera that share the same environment (e.g. coastal or offshore) have also accumulated shared and unique gene content that is predominantly involved in the metabolism of organic carbon and the acquisition of nitrogen from organic sources. A subset of these metabolic genes were under high purifying selection, emphasizing the importance of these functions to the fitness of distinct *Pelagibacteraceae* genera and highlighting potential determinants of niche differentiation of *Pelagibacteraceae* in coastal and offshore environments.

The cohesion of both ecological and genetic diversity observed within genera of *Pelagibacteraceae* most closely resembles ecotypes: ecologically homogeneous groups of closely related bacteria whose genetic diversity is guided by cohesive forces of selection, recombination, and genetic drift (Cohan 2006; Koeppel et al. 2008). Ecotypic differentiation has previously been suggested to describe the spatial and temporal variation partitioning genetic and genomic SAR11 diversity (Field et al. 1997; Schwalbach et al. 2010; Brown et al. 2012; Vergin et al. 2013; Tsementzi et al. 2019; Haro-Moreno et al. 2020; Kraemer et al. 2020; Tucker et al. 2021; Larkin et al. 2023; Freel et al. 2024), however the underlying evolutionary processes or functional differences contributing to this diversification have rarely been linked to patterns of distribution. Our findings reveal evolutionary drivers behind ecotypic differentiation by

548 explaining distinct ecological distribution patterns with differences in gene content, metabolic
549 potential, and selective pressures across ecotypes. The use of a constrained model system that
550 provided both metagenomic sequence data as well as isolate genomes from local
551 *Pelagibacteraceae* populations was paramount to being able to resolve signatures of
552 environmental selection in sympatric and parapatric SAR11 populations. The power of this
553 approach is further demonstrated in the fact that most of the *Pelagibacteraceae* ecotypes defined
554 in this constrained system as having preferences for coastal oceans or the open ocean appear to
555 hold when global read recruitment data were examined (Freel et al. 2024).

556 Our results suggest that *Pelagibacteraceae* has transitioned between offshore and coastal
557 environments multiple times, with a handful of genes that support these lifestyles likely acquired
558 through multiple independent processes. The small number of adaptive genes are shared among
559 ecologically similar, but polyphyletically-distributed genera, where genomes have maintained a
560 substantial amount of genetic diversity. Given the distribution patterns of the adaptive genes and
561 the genetic diversity maintained within the populations that carry them, the proliferation of
562 adaptive genes unlikely occurred via genome-wide selective sweep (Shapiro et al. 2016), a
563 process that describes the clonal expansion of an individual subpopulation that carries an
564 adaptive gene leading to a genome-wide reduction in genetic diversity. Instead, the maintenance
565 of genetic diversity and the relatively strong purifying selection to maintain the functional
566 identity of these adaptive genes is consistent with a gene-specific selective sweep (Falush et al.
567 2001; Whitaker et al. 2005; Shapiro et al. 2012; Rosen et al. 2015; Bendall et al. 2016).
568 Consistent with previous studies that have identified a handful of genes responsible for
569 habitat-specific adaptation (Shapiro et al. 2012; Bendall et al. 2016; Delmont and Eren 2018), the
570 gene content differences attributed to stable ecological speciation here are generally found within

571 the relatively stable genomic backbone, rather than within hyper-variable genomic islands. This
572 is a critical observation as it links eco-evolutionary processes to specific portions of the immense
573 genomic diversity that exists within *Pelagibacteraceae*, and underscores the importance of
574 analyses informed by genomic architecture. Future studies that examine the contribution of gene
575 content found within hyper-variable islands to stable ecological speciation as opposed to
576 incipient speciation or intraspecific diversity would provide a better understanding of the role of
577 hyper-variable regions in long-term evolutionary processes.

578 In closing, our analyses broaden the metabolic diversity known from *Pelagibacteraceae*
579 genomes and suggest that metabolic versatility has contributed to SAR11's success in the global
580 ocean. While metabolic reconstructions are subject to uncertainties that necessitate physiological
581 exploration with controlled experimentation in the laboratory, the metabolic analysis of
582 high-quality genomes from cultivated isolates provides the opportunity to delineate metabolic
583 specialization that could advance cultivation approaches and allow for more targeted media
584 recipes (Rappé et al. 2002; Stingl et al. 2007; Song et al. 2009; Henson et al. 2016). SAR11 is
585 estimated to oxidize between 6% to 37% of gross ocean primary productivity (White et al. 2019).
586 Future work combining these metabolic predictions with *in situ* measures will greatly improve
587 our understanding of how SAR11 impacts the dissolved organic matter pool and biogeochemical
588 cycles in the ocean.

Methods

Pangenome analyses

Publicly-available *Pelagibacteraceae* isolate genomes downloaded from the National Center for Biotechnology Information (NCBI) or the Joint Genome Institute (JGI) were combined with genomes sequenced from newly isolated strains (Freel et al. 2024; **Supplementary file 1a**). Genome completion and contamination were examined with checkM v1.1.2 (Parks et al. 2015) and only isolates above 95% completion with less than 5% redundancy (Bowers et al. 2017) and fewer than 50 contigs were kept (**Supplementary file 1a).** High-quality *Pelagibacteraceae* genomes were used to construct a pangenome using anvi'o v8.0 (Eren et al. 2021) following previously described pipelines (Delmont and Eren 2018). Briefly, an anvi'o database was created using `anvi-gen-contigs-db` and Prodigal v2.6.3 (Hyatt et al. 2010) was used to identify open reading frames (ORFs) from contigs. Single-copy core genes were identified using HMMER v3.2.1 (Eddy 2011). ORFs with associated functions were annotated from NCBI's Clusters of Orthologous Groups (COGs; Tatusov et al. 2003) and a customized HMM database of KEGG orthologs (KOfams; Kanehisa and Goto 2000; Aramaki et al. 2020). The pangenome was created with `anvi-pan-genome`, which uses NCBI's Basic Local Alignment Search Tool (BLAST; Altschul et al. 1990) to quantify the similarity between pairs of gene clusters and the Markov Cluster algorithm (MCL; Enright et al. 2002) to define homologous gene clusters with a MCL inflation parameter of 2. The pangenomes were visualized using the command `anvi-display-pan` and summary tables exported using the command `anvi-summarize`.

610 Genome-wide average nucleotide identity (gANI) was estimated using FastANI in anvi'o
611 (Jain et al. 2018). A phylogenomic tree of the *Pelagibacteraceae* was estimated using IQ-Tree
612 v2.12 (Minh et al. 2020) using 1000 ultrafast bootstraps and model LG+F+R10 from a
613 concatenated alignment of a custom gene set for SAR11 (SAR11_165; Freel et al. 2024).
614 Phylogenies were rooted and branches trimmed in R v 4.4.1 (R Core Team 2023) using treeio
615 v1.28.0 (Wang et al. 2020) and visulized in R using phytools v 2.3.0 (Revell 2012) to examine
616 the phylogenomic relationships between *Pelagibacteraceae* groups detected in our
617 environmental study.

618 Gene clusters found in 100% of *Pelagibacteraceae* genomes were considered core while
619 gene clusters found in only one genome were considered singletons. Gene clusters were also
620 assessed as genus specific (shared among all representatives of a genus and not found in other
621 genera) and multi-genus specific (shared among all representatives of two or more genera and
622 not found among all others). Shared gene content between genera was assessed using
623 ComplexUpset v 1.3.3 (Lex et al. 2014).

624 Metagenomic read recruitment and environmental analyses

625 To examine the distribution of *Pelagibacteraceae* genera within the environments from
626 where the majority were isolated, metagenomic read recruitment was conducted using surface
627 ocean metagenomes from 10 stations within and adjacent to Kānʻeohe Bay, Hawaiʻi (**Fig. 1**)
628 collected as part of the Kāneʻohe Bay Time-series (KByT; PRJNA971314; Tucker et al. 2021,
629 2024). In addition, metagenomes collected in the surrounding North Pacific Subtropical Gyre at
630 Station ALOHA, a sampling location within the Hawaii Ocean Time-series (**Fig. 1;**
631 **Supplementary file 1c**; PRJNA352737; Mende et al. 2017) were also used. Metagenomes were

632 competitively mapped with Bowtie2 v 2.3.5 (Langmead and Salzberg 2012) to the anvi'o contig
633 database of *Pelagibacteraceae* isolate genomes. The `anvi-profile` function stored coverage and
634 detection statistics of each *Pelagibacteraceae* genome found in the KByT and Station ALOHA
635 metagenomic samples and the `anvi-meta-pan-genome` function (Delmont and Eren 2018) was
636 used to bring together the pangenomic information with the read recruitment data.

637 To evaluate the distribution of individual genomes, a detection metric- the proportion of
638 the nucleotides in a given sequence that are covered by at least one short read- was used to define
639 whether a population was detected in a metagenomic sample. A detection value of at least 0.25
640 was used as criteria to eliminate false positives that could arise if an isolate genome was falsely
641 found within a sample (Utter et al. 2020).

642 The average depth of coverage excluding nucleotide positions with coverages in the 1st
643 and 4th quartiles (mean coverage Q2Q3) was mapped for each genome in each sample. To avoid
644 biased estimates of coverage that can occur due to highly recruiting accessory genes, read
645 recruitment was analyzed using only single-copy genes core to each genus. Using a custom script
646 in R, gene clusters that were found within all genomes of the genus (e.g. core), but found only in
647 a single copy within each genome were identified. Then the mean coverage Q2Q3 read
648 recruitment data per gene were then subsetted for only single copy core genes. The mean
649 coverage Q2Q3 of each single-copy core gene was summed per genome per sample and then this
650 value was normalized per genome per sample, based on whether the genome was detected at
651 >0.25 (Utter et al. 2020). Next, when evaluating read recruitment at the genus-level, the read
652 recruitment was summed for all genomes in a genus per sample. These outputs were then divided
653 across the total *Pelagibacteraceae* read recruitment for the sample to yield a relative estimate of
654 each genome or genus within a sample. For the genus with only a single genome representative

655 (*Semelpelagibacter*), the single-copy core genes shared with the HIMB1483 genome and nearest
656 neighbor, genus *Lacunapelagibacter*, were used.

657 K-means clustering analysis of a scaled matrix of biogeochemical conditions was used to
658 characterize the environmental background from which the metagenomic data were derived.
659 Metadata from Station ALOHA were downloaded from
660 https://hahana.soest.hawaii.edu/hot/hot-dogs/ (accessed 11 Oct 2021). All KByT (n=158) and
661 Station ALOHA (n=34) surface seawater samples (depth of <30m) with data for flow
662 cytometrically-determined cellular abundance, chlorophyll *a* concentrations, silicate
663 concentrations, temperature, pH, and salinity were included in the analyses (**Supplementary file**
664 **1c**). The number of clusters were estimated using the `kmeansruns` command in the R fpc v
665 2.2.13 package (Hennig 2024) using a Calinski Harabasz index. Principal Component Analysis
666 (PCA) was conducted using the `prcomp` function in R v 4.4.1 (R Core Team 2023) and
667 visualized using 'ggbiplot' in the ggplot2 v 3.5.1 (Wickham 2016).

668 The sampling locations of the Kāneʻohe Bay Time-series and Station ALOHA were
669 mapped using R with `geom_sf` from ggplot2 with geospatial data of the main Hawaiian Islands
670 (USGS Digital Line Graphs). To visualize *Prochlorococcus* cellular abundance across the
671 Kāneʻohe Bay Time-series, `mba.surf` from MBA v 0.1.2 (Finley et al. 2017) was used to
672 interpolate data over the KByT stations.

673 Functional inferences from *Pelagibacteraceae* genera

674 Functional enrichment analysis was performed in anvi'o and has been described
675 previously (Shaiber et al. 2020). Briefly, the `anvi-compute-functional-enrichment` command,
676 as well as the `anvi-script-gen-function-matrix-across-genomes`, was used to assess the

677 enrichment of Clusters of Orthologous Groups (COG), KEGG orthologs (KOs), and KEGG
678 modules across genomes and genus affiliations. The degree of completeness of individual KEGG
679 modules (Kanehisa et al. 2014, 2017) in the genomes and genera was evaluated using
680 `anvi-estimate-metabolism` (Veseli et al. 2023), prior to `anvi-compute-functional-enrichment`.
681 The functional pangenome was visualized using `anvi-display-functions`. Central and
682 alternative carbon metabolisms, amino acid, vitamin, and cofactor biosynthesis, and genes to
683 cope with nutrient, osmotic, and oxidative stress were examined across the *Pelagibacteraceae*
684 isolate genomes. The distribution of functional genes were evaluated for each genus as follows:
685 core genes found in all genomes of a genus, intermediate genes found in 15-99% of genomes,
686 and rare genes found in less than 15%. Heatmaps of the metabolic gene distribution across
687 genera were made in the R package pheatmap v 1.0.12 (Kolde 2019).

688 Selection within *Pelagibacteraceae* genes

689 To evaluate the selective pressures on individual metabolic genes of interest, the
690 proportion of non-synonymous to synonymous (pN/pS) sites per gene across genomes was
691 evaluated. The pipeline followed those developed in Kiefl et al., (2023). Briefly, contig databases
692 from the genomes of type specimens from each of the *Pelagibacteraceae* genera (Freel et al.
693 2024) were first functionally annotated in anvi'o (see above) and metagenomic reads from
694 deeply sequenced metagenomes from either coastal Kāneʻohe Bay or the adjacent offshore were
695 non-competitively recruited using Bowtie2 v 2.3.5 (Langmead and Salzberg 2012;
696 **Supplementary file 1c**).
697 Next, the`anvi-profile` function with the flag `--profile-SCVs` was used to characterize
698 single codon variants across the read recruitment data and then `anvi-gen-variability-profile`

was used to export the single codon variants per gene per sample using the flags --engine CDN --include-site-pN/pS --kiefl-mode (Kiefl et al. 2023). Finally, pN/pS values were reported per gene with at least 20x coverage in each sample using 'anvi-get-pn-ps-ratio` with the -m 20 flag. Per gene coverage statistics were exported using `anvi-summarize` with the `--init-gene-coverages` flag. Functional annotations were exported using `anvi-export-functions`.

To evaluate whether a single genome representative contained similar pN/pS gene values as other genomes within a given genus, these steps were repeated with all representatives of the genus sharing the lowest minimum gANI (among the genera that were abundant in the tropical Pacific): genus *Coralipelagibacter*. The exported data files were brought into R, where variation in pN/pS per sample, per genome, and across genomes of the same genus was evaluated. Relationships between pN/pS and coverage were examined and genes per genome representative were ranked from lowest pN/pS value to highest and visualized in R using ggplot2 v 3.5.1 (Wickham 2016). Figures were made in R v 4.4.1 (R Core Team 2023) or anvi'o (Eren et al. 2021) and further edited with Inkscape (https://inkscape.org/).

Data availability

Accession numbers for genome sequences used to conduct pangenomic analyses and read recruitment in this study are found in **Supplementary file 1a**. Short-read metagenome accession IDs and environmental data used in this study are provided in **Supplementary file 1c**. Long-read metagenomes from coastal Kāneʻohe Bay are available under NCBI Project PRJNA1201851.

Code availability

Code to run analyses and create figures can be found at https://github.com/tucker4/SAR11_metabolism.

Competing interests

The authors declare no competing interests.

Acknowledgements

We thank Oscar Ramfelt and Evan B. Freel for their insights on computational analyses. This research was funded by the Simons Postdoctoral Fellowships in Marine Microbial Ecology (grant #989028), NOAA Margaret A. Davidson Fellowship, the Colonel Willys E. Lord, DVM and Sadina L. Lord Scholarship, the ARCS Foundation George Orton and Mona Marie Elmore Award in Marine Biology, the Research Corporation of the University of Hawai‘i Graduate Research Fellowship, the EECB Hampton and Meredith Carson Fellowship, and the Center for Microbial Analysis through Island Knowledge & Investigation Research Grant to SJ Tucker, and NSF grants OCE-1538628 and OCE- 2149128 to MS Rappé. AME acknowledges support from the Center for Chemical Currencies of a Microbial Planet (C-CoMP) (NSF Award OCE-2019589, C-CoMP publication #065), and Simons Foundation (grant #687269)

References

Acker, M., S. L. Hogle, P. M. Berube, T. Hackl, A. Coe, R. Stepanauskas, S. W. Chisholm, and D. J. Repeta. 2022. Phosphonate production by marine microbes: Exploring new sources and potential function. Proc. Natl. Acad. Sci. U. S. A. **119**: e2113386119. doi:10.1073/pnas.2113386119

Altschul, S. F., W. Gish, W. Miller, E. W. Myers, and D. J. Lipman. 1990. Basic local alignment search tool. J. Mol. Biol. **215**: 403–410. doi:10.1016/S0022-2836(05)80360-2

Aramaki, T., R. Blanc-Mathieu, H. Endo, K. Ohkubo, M. Kanehisa, S. Goto, and H. Ogata. 2020. KofamKOALA: KEGG Ortholog assignment based on profile HMM and adaptive score threshold. Bioinformatics **36**: 2251–2252. doi:10.1093/bioinformatics/btz859

Bendall, M. L. and others. 2016. Genome-wide selective sweeps and gene-specific sweeps in natural bacterial populations. ISME J. **10**: 1589–1601. doi:10.1038/ismej.2015.241

Berman, T., and D. A. Bronk. 2003. Dissolved organic nitrogen: a dynamic participant in aquatic ecosystems. Aquat. Microb. Ecol. **31**: 279–305. doi:10.3354/ame031279

Bowers, R. M. and others. 2017. Minimum information about a single amplified genome (MISAG) and a metagenome-assembled genome (MIMAG) of bacteria and archaea. Nat. Biotechnol. **35**: 725–731. doi:10.1038/nbt.3893

Braakman, R. and others. 2024. Global niche partitioning of purine and pyrimidine cross-feeding among ocean microbes. bioRxiv. doi:10.1101/2024.02.09.579562

Braakman, R., M. J. Follows, and S. W. Chisholm. 2017. Metabolic evolution and the self-organization of ecosystems. Proc. Natl. Acad. Sci. U. S. A. **114**: E3091–E3100. doi:10.1073/pnas.1619573114

Brown, M. V. and others. 2012. Global biogeography of SAR11 marine bacteria. Mol. Syst. Biol. **8**: 595. doi:10.1038/msb.2012.28

Castell, C., L. A. Rodríguez-Lumbreras, M. Hervás, J. Fernández-Recio, and J. A. Navarro. 2021. New insights into the evolution of the electron transfer from cytochrome f to photosystem I in the Green

and red branches of photosynthetic eukaryotes. Plant Cell Physiol. **62**: 1082–1093. doi:10.1093/pcp/pcab044

Clifton, B. E., U. Alcolombri, G.-I. Uechi, C. J. Jackson, and P. Laurino. 2024. The ultra-high affinity transport proteins of ubiquitous marine bacteria. Nature **634**: 721–728. doi:10.1038/s41586-024-07924-w

Cohan, F. M. 2006. Towards a conceptual and operational union of bacterial systematics, ecology, and evolution. Philos. Trans. R. Soc. Lond. B Biol. Sci. **361**: 1985–1996. doi:10.1098/rstb.2006.1918

Conrad, R. E., T. Viver, J. F. Gago, J. K. Hatt, S. N. Venter, R. Rossello-Mora, and K. T. Konstantinidis. 2022. Toward quantifying the adaptive role of bacterial pangenomes during environmental perturbations. ISME J. **16**: 1222–1234. doi:10.1038/s41396-021-01149-9

Cordero, O. X., and M. F. Polz. 2014. Explaining microbial genomic diversity in light of evolutionary ecology. Nat. Rev. Microbiol. **12**: 263–273. doi:10.1038/nrmicro3218

Delmont, T. O., and A. M. Eren. 2018. Linking pangenomes and metagenomes: the Prochlorococcus metapangenome. PeerJ **6**: e4320. doi:10.7717/peerj.4320

Delmont, T. O., E. Kiefl, O. Kilinc, O. C. Esen, I. Uysal, M. S. Rappé, S. Giovannoni, and A. M. Eren. 2019. Single-amino acid variants reveal evolutionary processes that shape the biogeography of a global SAR11 subclade. Elife **8**. doi:10.7554/elife.46497

Doyle, M. T., E. N. H. Tran, and R. Morona. 2015. The passenger-associated transport repeat promotes virulence factor secretion efficiency and delineates a distinct autotransporter subtype. Mol. Microbiol. **97**: 315–329. doi:10.1111/mmi.13027

Eddy, S. R. 2011. Accelerated profile HMM searches. PLoS Comput. Biol. **7**: e1002195. doi:10.1371/journal.pcbi.1002195

Ellison, C. K., T. N. Dalia, A. Vidal Ceballos, J. C.-Y. Wang, N. Biais, Y. V. Brun, and A. B. Dalia. 2018. Retraction of DNA-bound type IV competence pili initiates DNA uptake during natural transformation in Vibrio cholerae. Nat. Microbiol. **3**: 773–780. doi:10.1038/s41564-018-0174-y

Enright, A. J., S. Van Dongen, and C. A. Ouzounis. 2002. An efficient algorithm for large-scale detection

of protein families. Nucleic Acids Res. **30**: 1575–1584. doi:10.1093/nar/30.7.1575

Eren, A. M. and others. 2021. Community-led, integrated, reproducible multi-omics with anvi'o. Nat. Microbiol. **6**: 3–6. doi:10.1038/s41564-020-00834-3

Falush, D., C. Kraft, N. S. Taylor, P. Correa, J. G. Fox, M. Achtman, and S. Suerbaum. 2001. Recombination and mutation during long-term gastric colonization by Helicobacter pylori: estimates of clock rates, recombination size, and minimal age. Proc. Natl. Acad. Sci. U. S. A. **98**: 15056–15061. doi:10.1073/pnas.251396098

Field, K. G., D. Gordon, T. Wright, M. Rappé, E. Urback, K. Vergin, and S. J. Giovannoni. 1997. Diversity and depth-specific distribution of SAR11 cluster rRNA genes from marine planktonic bacteria. Appl. Environ. Microbiol. **63**: 63–70. doi:10.1128/aem.63.1.63-70.1997

Finley, A., S. Banerjee, and Ø. Hjelle. 2017. MBA: Multilevel B-Spline Approximation. R package version 0.1-2,.

Freel, K. C., S. J. Tucker, E. B. Freel, S. J. Giovannoni, A. M. Eren, and M. S. Rappe. 2024. New isolate genomes and global marine metagenomes resolve ecologically relevant units of SAR11. bioRxiv 2024.12.24.630191. doi:10.1101/2024.12.24.630191

Giovannoni, S. J. and others. 2005. Genome streamlining in a cosmopolitan oceanic bacterium. Science **309**: 1242–1245. doi:10.1126/science.1114057

Giovannoni, S. J. 2017. SAR11 bacteria: The most abundant plankton in the oceans. Ann. Rev. Mar. Sci. **9**: 231–255. doi:10.1146/annurev-marine-010814-015934

Giovannoni, S. J., J. Cameron Thrash, and B. Temperton. 2014. Implications of streamlining theory for microbial ecology. ISME J. **8**: 1553–1565. doi:10.1038/ismej.2014.60

Gralka, M., S. Pollak, and O. X. Cordero. 2023. Genome content predicts the carbon catabolic preferences of heterotrophic bacteria. Nat. Microbiol. **8**: 1799–1808. doi:10.1038/s41564-023-01458-z

Grant, S. R., M. J. Church, S. Ferrón, E. A. Laws, and M. S. Rappé. 2019. Elemental composition, phosphorous uptake, and characteristics of growth of a SAR11 strain in batch and continuous culture. mSystems **4**. doi:10.1128/msystems.00218-18

Grote, J., J. C. Thrash, M. J. Huggett, Z. C. Landry, P. Carini, S. J. Giovannoni, and M. S. Rappé. 2012. Streamlining and core genome conservation among highly divergent members of the SAR11 clade. MBio **3**. doi:10.1128/mbio.00252-12

Hao, L., T. Y. Michaelsen, C. M. Singleton, G. Dottorini, R. H. Kirkegaard, M. Albertsen, P. H. Nielsen, and M. S. Dueholm. 2020. Novel syntrophic bacteria in full-scale anaerobic digesters revealed by genome-centric metatranscriptomics. ISME J. **14**: 906–918. doi:10.1038/s41396-019-0571-0

Haro-Moreno, J. M. and others. 2020. Ecogenomics of the SAR11 clade. Environ. Microbiol. **22**: 1748–1763. doi:10.1111/1462-2920.14896

Hazes, B., and L. Frost. 2008. Towards a systems biology approach to study type II/IV secretion systems. Biochim. Biophys. Acta **1778**: 1839–1850. doi:10.1016/j.bbamem.2008.03.011

Hennig, C. 2024. fpc: Flexible procedures for clustering. R package version 2.2-13,.

Henson, M. W., D. M. Pitre, J. L. Weckhorst, V. C. Lanclos, A. T. Webber, and J. C. Thrash. 2016. Artificial seawater media facilitate cultivating members of the microbial majority from the Gulf of Mexico. mSphere **1**. doi:10.1128/mSphere.00028-16

Hyatt, D., G.-L. Chen, P. F. Locascio, M. L. Land, F. W. Larimer, and L. J. Hauser. 2010. Prodigal: prokaryotic gene recognition and translation initiation site identification. BMC Bioinformatics **11**: 119. doi:10.1186/1471-2105-11-119

Jain, C., L. M. Rodriguez-R, A. M. Phillippy, K. T. Konstantinidis, and S. Aluru. 2018. High throughput ANI analysis of 90K prokaryotic genomes reveals clear species boundaries. Nat. Commun. **9**: 5114. doi:10.1038/s41467-018-07641-9

Kanehisa, M., M. Furumichi, M. Tanabe, Y. Sato, and K. Morishima. 2017. KEGG: new perspectives on genomes, pathways, diseases and drugs. Nucleic Acids Res. **45**: D353–D361. doi:10.1093/nar/gkw1092

Kanehisa, M., and S. Goto. 2000. KEGG: kyoto encyclopedia of genes and genomes. Nucleic Acids Res. **28**: 27–30. doi:10.1093/nar/28.1.27

Kanehisa, M., S. Goto, Y. Sato, M. Kawashima, M. Furumichi, and M. Tanabe. 2014. Data, information,

knowledge and principle: back to metabolism in KEGG. Nucleic Acids Res. **42**: D199–205. doi:10.1093/nar/gkt1076

Kiefl, E., O. C. Esen, S. E. Miller, K. L. Kroll, A. D. Willis, M. S. Rappé, T. Pan, and A. M. Eren. 2023. Structure-informed microbial population genetics elucidate selective pressures that shape protein evolution. Sci Adv **9**: eabq4632. doi:10.1126/sciadv.abq4632

Klähn, S., C. Steglich, W. R. Hess, and M. Hagemann. 2010. Glucosylglycerate: a secondary compatible solute common to marine cyanobacteria from nitrogen-poor environments. Environ. Microbiol. **12**: 83–94. doi:10.1111/j.1462-2920.2009.02045.x

Koeppel, A. and others. 2008. Identifying the fundamental units of bacterial diversity: a paradigm shift to incorporate ecology into bacterial systematics. Proc. Natl. Acad. Sci. U. S. A. **105**: 2504–2509. doi:10.1073/pnas.0712205105

Kolde, R. 2019. pheatmap: Pretty Heatmaps. R package version 1.0.12,.

Kornberg, R. D. 1974. Chromatin structure: a repeating unit of histones and DNA. Science **184**: 868–871. doi:10.1126/science.184.4139.868

Kraemer, S., A. Ramachandran, D. Colatriano, C. Lovejoy, and D. A. Walsh. 2020. Diversity and biogeography of SAR11 bacteria from the Arctic Ocean. ISME J. **14**: 79–90. doi:10.1038/s41396-019-0499-4

Langmead, B., and S. L. Salzberg. 2012. Fast gapped-read alignment with Bowtie 2. Nat. Methods **9**: 357–359. doi:10.1038/nmeth.1923

Larkin, A. A., G. I. Hagstrom, M. L. Brock, N. S. Garcia, and A. C. Martiny. 2023. Basin-scale biogeography of Prochlorococcus and SAR11 ecotype replication. ISME J. **17**: 185–194. doi:10.1038/s41396-022-01332-6

Lex, A., N. Gehlenborg, H. Strobelt, R. Vuillemot, and H. Pfister. 2014. UpSet: Visualization of intersecting sets. IEEE Trans. Vis. Comput. Graph. **20**: 1983–1992. doi:10.1109/TVCG.2014.2346248

Leyton, D. L., A. E. Rossiter, and I. R. Henderson. 2012. From self sufficiency to dependence:

mechanisms and factors important for autotransporter biogenesis. Nat. Rev. Microbiol. **10**: 213–225. doi:10.1038/nrmicro2733

Louca, S. and others. 2016. Integrating biogeochemistry with multiomic sequence information in a model oxygen minimum zone. Proc. Natl. Acad. Sci. U. S. A. **113**: E5925–E5933. doi:10.1073/pnas.1602897113

Mende, D. R., J. A. Bryant, F. O. Aylward, J. M. Eppley, T. Nielsen, D. M. Karl, and E. F. DeLong. 2017. Environmental drivers of a microbial genomic transition zone in the ocean's interior. Nat. Microbiol. **2**: 1367–1373. doi:10.1038/s41564-017-0008-3

Meuskens, I., A. Saragliadis, J. C. Leo, and D. Linke. 2019. Type V secretion systems: An overview of passenger domain functions. Front. Microbiol. **10**: 1163. doi:10.3389/fmicb.2019.01163

Minh, B. Q., H. A. Schmidt, O. Chernomor, D. Schrempf, M. D. Woodhams, A. von Haeseler, and R. Lanfear. 2020. IQ-TREE 2: New models and efficient methods for phylogenetic inference in the genomic era. Mol. Biol. Evol. **37**: 1530–1534. doi:10.1093/molbev/msaa015

Moore, E. R., A. J. Weaver, E. W. Davis, S. J. Giovannoni, and K. H. Halsey. 2022. Metabolism of key atmospheric volatile organic compounds by the marine heterotrophic bacterium Pelagibacter HTCC1062 (SAR11). Environ. Microbiol. **24**: 212–222. doi:10.1111/1462-2920.15837

Morris, J. J., R. E. Lenski, and E. R. Zinser. 2012. The Black Queen Hypothesis: evolution of dependencies through adaptive gene loss. MBio **3**. doi:10.1128/mBio.00036-12

Morris, R. M., M. S. Rappé, S. A. Connon, K. L. Vergin, W. A. Siebold, C. A. Carlson, and S. J. Giovannoni. 2002. SAR11 clade dominates ocean surface bacterioplankton communities. Nature **420**: 806–810. doi:10.1038/nature01240

Noell, S. E., E. Brennan, Q. Washburn, E. W. Davis 2nd, F. L. Hellweger, and S. J. Giovannoni. 2023. Differences in the regulatory strategies of marine oligotrophs and copiotrophs reflect differences in motility. Environ. Microbiol. **25**: 1265–1280. doi:10.1111/1462-2920.16357

Noell, S. E., and S. J. Giovannoni. 2019. SAR11 bacteria have a high affinity and multifunctional glycine betaine transporter. Environ. Microbiol. **21**: 2559–2575. doi:10.1111/1462-2920.14649

Parks, D. H., M. Imelfort, C. T. Skennerton, P. Hugenholtz, and G. W. Tyson. 2015. CheckM: assessing the quality of microbial genomes recovered from isolates, single cells, and metagenomes. Genome Res. **25**: 1043–1055. doi:10.1101/gr.186072.114

Peers, G., and N. M. Price. 2006. Copper-containing plastocyanin used for electron transport by an oceanic diatom. Nature **441**: 341–344. doi:10.1038/nature04630

Rappé, M. S., S. A. Connon, K. L. Vergin, and S. J. Giovannoni. 2002. Cultivation of the ubiquitous SAR11 marine bacterioplankton clade. Nature **418**: 630–633. doi:10.1038/nature00917

R Core Team. 2023. R: A language and environment for statistical computing,.

Ren, D., B. Navarro, H. Xu, L. Yue, Q. Shi, and D. E. Clapham. 2001. A prokaryotic voltage-gated sodium channel. Science **294**: 2372–2375. doi:10.1126/science.1065635

Revell, L. J. 2012. phytools: an R package for phylogenetic comparative biology (and other things). Methods Ecol. Evol. **3**: 217–223. doi:10.1111/j.2041-210x.2011.00169.x

Rosen, M. J., M. Davison, D. Bhaya, and D. S. Fisher. 2015. Microbial diversity. Fine-scale diversity and extensive recombination in a quasisexual bacterial population occupying a broad niche. Science **348**: 1019–1023. doi:10.1126/science.aaa4456

Schwalbach, M. S., H. J. Tripp, L. Steindler, D. P. Smith, and S. J. Giovannoni. 2010. The presence of the glycolysis operon in SAR11 genomes is positively correlated with ocean productivity. Environ. Microbiol. **12**: 490–500. doi:10.1111/j.1462-2920.2009.02092.x

Shaiber, A. and others. 2020. Functional and genetic markers of niche partitioning among enigmatic members of the human oral microbiome. Genome Biol. **21**: 292. doi:10.1186/s13059-020-02195-w

Shapiro, B. J., J. Friedman, O. X. Cordero, S. P. Preheim, S. C. Timberlake, G. Szabó, M. F. Polz, and E. J. Alm. 2012. Population genomics of early events in the ecological differentiation of bacteria. Science **336**: 48–51. doi:10.1126/science.1218198

Shapiro, B. J., J.-B. Leducq, and J. Mallet. 2016. What is speciation? PLoS Genet. **12**: e1005860. doi:10.1371/journal.pgen.1005860

Sheppard, S. K., D. S. Guttman, and J. R. Fitzgerald. 2018. Population genomics of bacterial host

adaptation. Nat. Rev. Genet. **19**: 549–565. doi:10.1038/s41576-018-0032-z

Smith, D. P., C. D. Nicora, P. Carini, M. S. Lipton, A. D. Norbeck, R. D. Smith, and S. J. Giovannoni. 2016. Proteome Remodeling in Response to Sulfur Limitation in "Candidatus Pelagibacter ubique." mSystems **1**. doi:10.1128/mSystems.00068-16

Song, J., H.-M. Oh, and J.-C. Cho. 2009. Improved culturability of SAR11 strains in dilution-to-extinction culturing from the East Sea, West Pacific Ocean. FEMS Microbiol. Lett. **295**: 141–147. doi:10.1111/j.1574-6968.2009.01623.x

Stingl, U., H. J. Tripp, and S. J. Giovannoni. 2007. Improvements of high-throughput culturing yielded novel SAR11 strains and other abundant marine bacteria from the Oregon coast and the Bermuda Atlantic Time Series study site. ISME J. **1**: 361–371. doi:10.1038/ismej.2007.49

Strege, P. R., L. M. Cowan, C. Alcaino, A. Mazzone, C. A. Ahern, L. S. Milescu, G. Farrugia, and A. Beyder. 2023. Mechanosensitive pore opening of a prokaryotic voltage-gated sodium channel. Elife **12**. doi:10.7554/eLife.79271

Sun, J., L. Steindler, J. C. Thrash, K. H. Halsey, D. P. Smith, A. E. Carter, Z. C. Landry, and S. J. Giovannoni. 2011. One carbon metabolism in SAR11 pelagic marine bacteria. PLoS One **6**: e23973. doi:10.1371/journal.pone.0023973

Tatusov, R. L. and others. 2003. The COG database: an updated version includes eukaryotes. BMC Bioinformatics **4**: 41. doi:10.1186/1471-2105-4-41

Tripp, H. J., J. B. Kitner, M. S. Schwalbach, J. W. H. Dacey, L. J. Wilhelm, and S. J. Giovannoni. 2008. SAR11 marine bacteria require exogenous reduced sulphur for growth. Nature **452**: 741–744. doi:10.1038/nature06776

Tripp, H. J., M. S. Schwalbach, M. M. Meyer, J. B. Kitner, R. R. Breaker, and S. J. Giovannoni. 2009. Unique glycine-activated riboswitch linked to glycine-serine auxotrophy in SAR11. Environ. Microbiol. **11**: 230–238. doi:10.1111/j.1462-2920.2008.01758.x

Tsementzi, D., L. M. Rodriguez-R, C. A. Ruiz-Perez, A. Meziti, J. K. Hatt, and K. T. Konstantinidis. 2019. Ecogenomic characterization of widespread, closely-related SAR11 clades of the freshwater

genus “Candidatus Fonsibacter” and proposal of Ca. Fonsibacter lacus sp. nov. Syst. Appl. Microbiol. **42**: 495–505. doi:10.1016/j.syapm.2019.03.007

Tucker, S. J., K. C. Freel, E. A. Monaghan, C. E. S. Sullivan, O. Ramfelt, Y. M. Rii, and M. S. Rappé. 2021. Spatial and temporal dynamics of SAR11 marine bacteria across a nearshore to offshore transect in the tropical Pacific Ocean. PeerJ **9**: e12274. doi:10.7717/peerj.12274

Tucker, S. J., Y. M. Rii, K. C. Freel, K. Kotubetey, A. H. Kawelo, K. B. Winter, and M. S. Rappe. 2024. Sharp transitions in phytoplankton communities across estuarine to open ocean waters of the tropical Pacific. bioRxiv. doi:10.1101/2024.05.23.595464

Utter, D. R., G. G. Borisy, A. M. Eren, C. M. Cavanaugh, and J. L. Mark Welch. 2020. Metapangenomics of the oral microbiome provides insights into habitat adaptation and cultivar diversity. Genome Biol. **21**: 293. doi:10.1186/s13059-020-02200-2

Vergin, K. L. and others. 2013. High-resolution SAR11 ecotype dynamics at the Bermuda Atlantic Time-series Study site by phylogenetic placement of pyrosequences. ISME J. **7**: 1322–1332. doi:10.1038/ismej.2013.32

Vergin, K. L., H. J. Tripp, L. J. Wilhelm, D. R. Denver, M. S. Rappé, and S. J. Giovannoni. 2007. High intraspecific recombination rate in a native population of Candidatus pelagibacter ubique (SAR11). Environ. Microbiol. **9**: 2430–2440. doi:10.1111/j.1462-2920.2007.01361.x

Veseli, I. and others. 2023. Microbes with higher metabolic independence are enriched in human gut microbiomes under stress.doi:10.7554/elife.89862

Wang, C., Q.-Y. Yu, N.-N. Ji, Y. Zheng, J. W. Taylor, L.-D. Guo, and C. Gao. 2023. Bacterial genome size and gene functional diversity negatively correlate with taxonomic diversity along a pH gradient. Nat. Commun. **14**: 7437. doi:10.1038/s41467-023-43297-w

Wang, L.-G. and others. 2020. Treeio: An R package for phylogenetic tree input and output with richly annotated and associated data. Mol. Biol. Evol. **37**: 599–603. doi:10.1093/molbev/msz240

Whelan, F. J., R. J. Hall, and J. O. McInerney. 2021. Evidence for selection in the abundant accessory gene content of a prokaryote pangenome. Mol. Biol. Evol. **38**: 3697–3708.

doi:10.1093/molbev/msab139

Whitaker, R. J., D. W. Grogan, and J. W. Taylor. 2005. Recombination shapes the natural population structure of the hyperthermophilic archaeon Sulfolobus islandicus. Mol. Biol. Evol. **22**: 2354–2361. doi:10.1093/molbev/msi233

White, A. E., S. J. Giovannoni, Y. Zhao, K. Vergin, and C. A. Carlson. 2019. Elemental content and stoichiometry of SAR11 chemoheterotrophic marine bacteria. Limnol. Oceanogr. Lett. **4**: 44–51. doi:10.1002/lol2.10103

Wickham, H. 2016. ggplot2: Elegant graphics for data analysis. Springer-Verlag New York,.

Yeo, S. K., M. J. Huggett, A. Eiler, and M. S. Rappé. 2013. Coastal bacterioplankton community dynamics in response to a natural disturbance. PLoS One **8**: e56207. doi:10.1371/journal.pone.0056207

Zhang, Y., and V. N. Gladyshev. 2008. Molybdoproteomes and evolution of molybdenum utilization. J. Mol. Biol. **379**: 881–899. doi:10.1016/j.jmb.2008.03.051

Zhao, X., C. L. Schwartz, J. Pierson, S. J. Giovannoni, J. R. McIntosh, and D. Nicastro. 2017. Three-Dimensional Structure of the Ultraoligotrophic Marine Bacterium “Candidatus Pelagibacter ubique.” Appl. Environ. Microbiol. **83**. doi:10.1128/aem.02807-16

Extended Data Figures

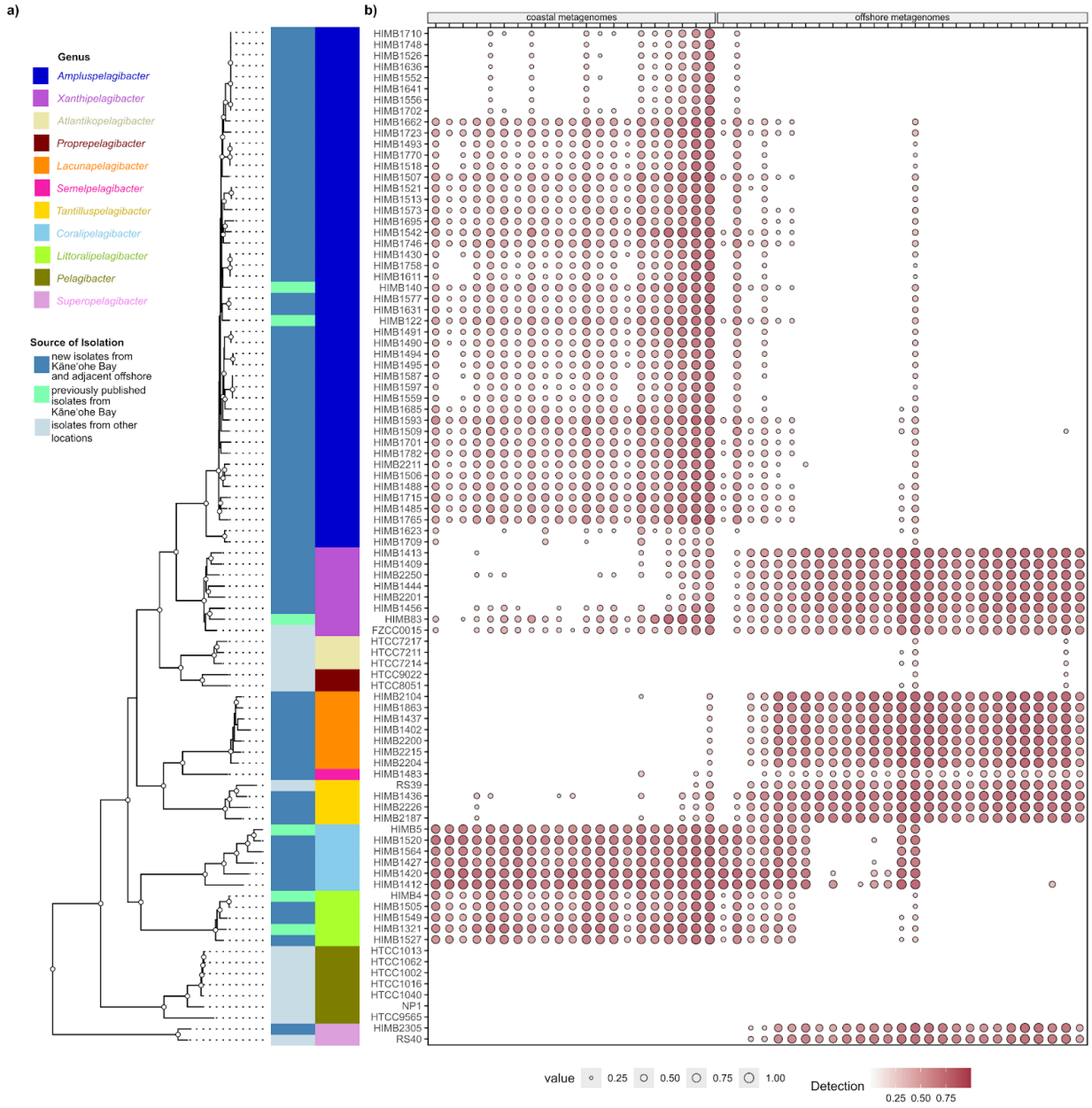

Extended Data Fig. 1. a) Phylogenomic tree showing 11 monophyletic clusters within *Pelagibacteraceae*, their genus assignments, and source of isolation. Circles at nodes indicate ultrafast bootstrap support values ≥90% from 1000 replicates. **b)** Detection of all *Pelagibacteraceae* genomes in coastal and offshore metagenomic samples.

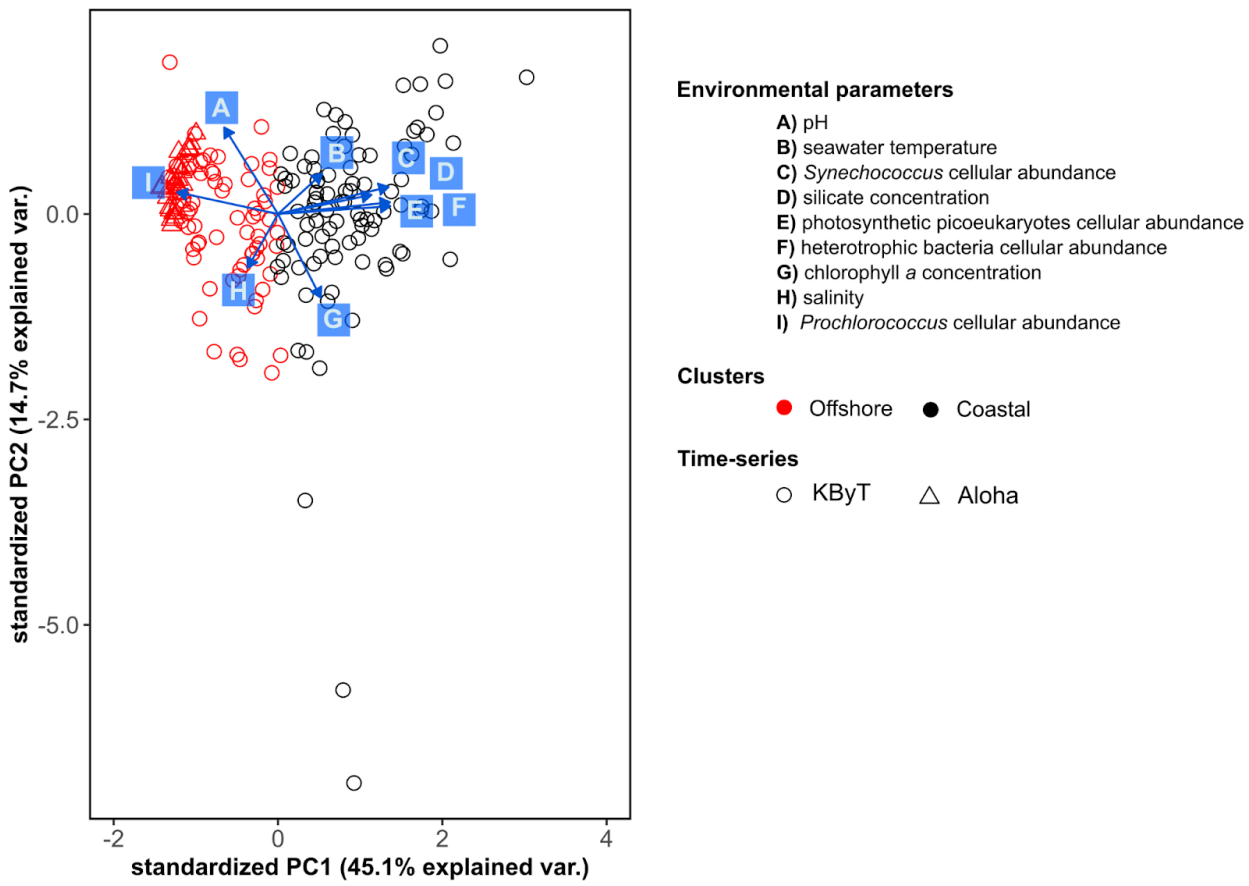

Extended Data Fig. 2. K-means analyses of environmental parameters from 192 surface ocean samples from KByT and Station ALOHA grouped into two clusters, herein referred to as coastal and offshore.

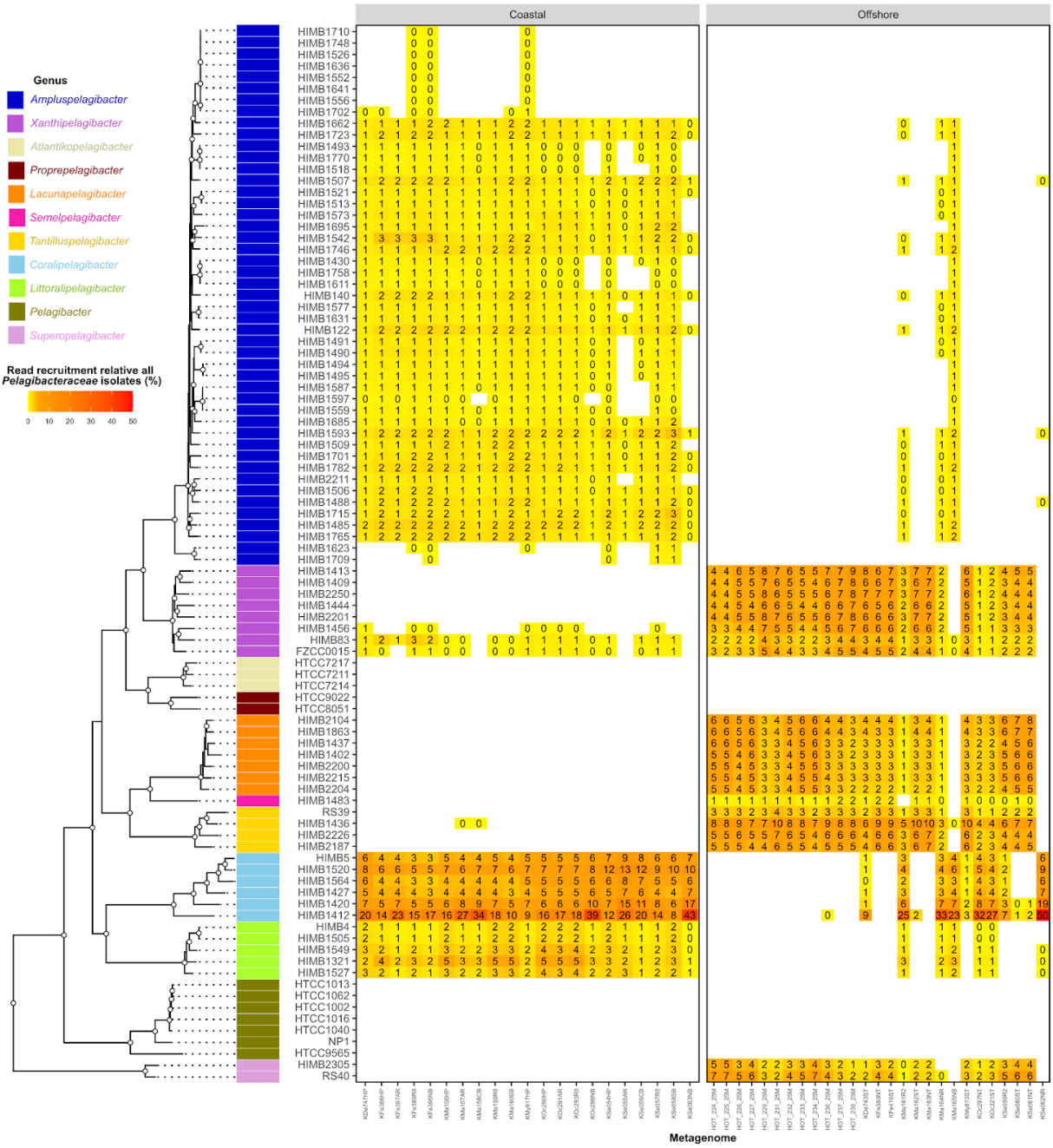

Extended Data Fig. 3. Relative read recruitment of each isolate genome across the coastal and offshore environment. Data for genomes that are not detected or have a relative recruitment less than 0.25% are not shown.

Extended Data Fig. 4. **a)** A protein structure model of a gene annotated as an autotransporter adhesin from KByT long-read metagenomes and sharing close sequence similarity to gene sequences in *Pelagibacteraceae* genomes shows characteristics expected of autotransporter proteins: 1) α-helical linker, 2) β-barrel translocator domain, and 3) passenger domains containing β helices (Leyton et al., 2012). **b)** Homolog searches to recover autotransporter adhesin genes in long-read metagenomes recovered nine non-redundant gene sequences that were near exact matches to most gene sequences in *Pelagibacteraceae* genomes (33 of 43). **c)**

Patterns of detection of short-read metagenomic read recruitment data across genes in two genomes of *Pelagibacteraceae* show that autotransporter adhesion genes are sometimes located in hypervariable regions and sometimes not. Genes for each *Pelagibacteraceae* genome are ordered by genome synteny with detection values of read recruitment data per gene shown as a bar per metagenomic sample. Areas of low detection are indicative of hypervariable regions (HVRs), and the autotransporter adhesin genes were located in HVRs within the HIMB5 genome, but not within HIMB4 genome. The autotransport adhesion genes were always positioned next to genes involved in type IV pilus systems and/or type II secretory systems.

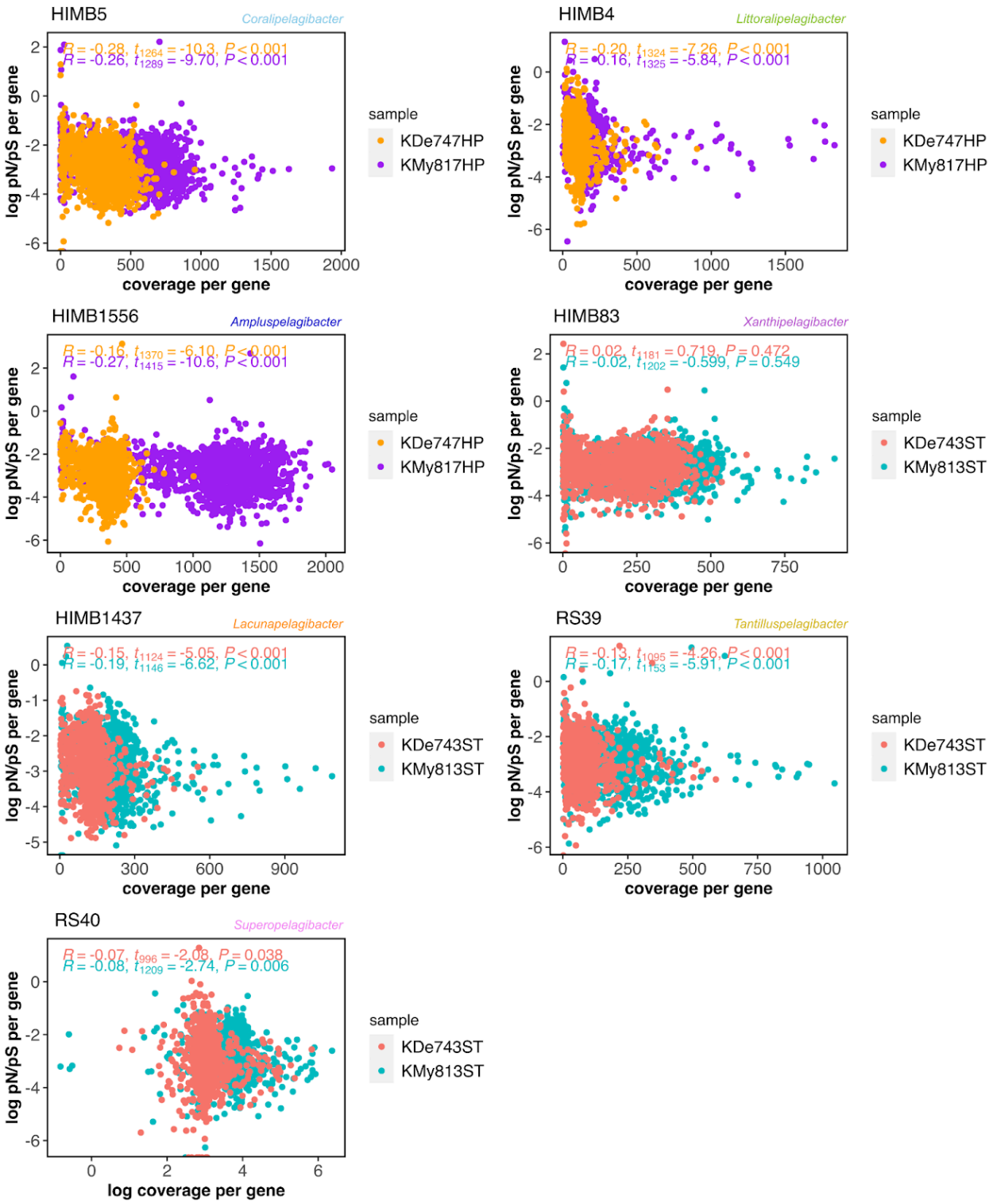

Extended Data Fig. 5. The coverage of genes from metagenomic read recruitment did not correlate with the pN/pS values. pN/pS: proportion of non-synonymous to synonymous.

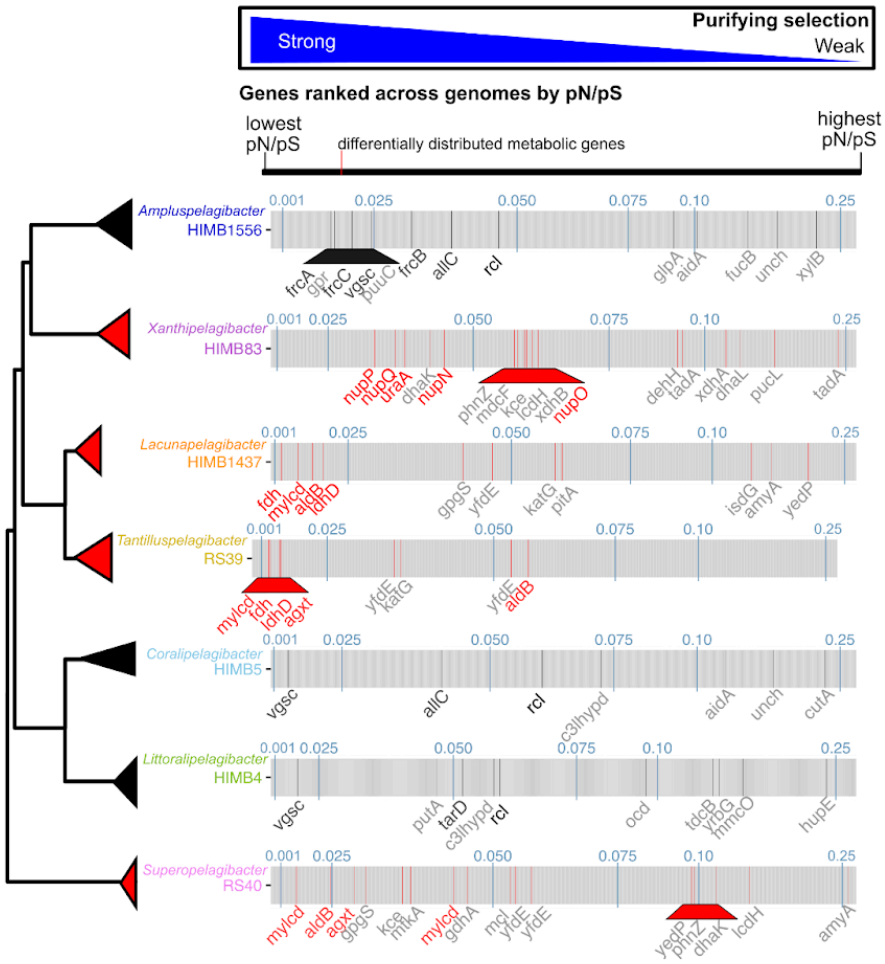

aidA	fibronectin-binding autotransporter adhesin
agxt	transaminase
aldB	aldehyde dehydrogenase
allC	allantoate deiminase
amyA	glycosidase/amylase
c3lhypd	cis-L-3-hydroxyproline dehydratase
cutA	copper tolerance
dehH	haloacetate dehalogenase
dhaK, dhaL	phosphoenolpyruvate: glycerone phosphotransferase
fdh	formate dehydrogenase
frcABC	fructose transport system
fucB	L-fuconolactonase
gdhA	glutamate dehydrogenase
glpA	glycerol-3-phosphate dehydrogenase
gpgS, yedP	glucosylglycerate synthesis
pucL	uric acid degradation
putA	proline dehydrogenase
puuC	putrescine glutamylation
rcl	nucleoside 2-deoxyribosyltransferase
tadA	tRNA adenosine deaminase
tarD	D-tartrate dehydratase
tdcB	threonine dehydratase
unch	n terminal nucleophile
uraA	xanthine permease
vgsc	voltage-gated sodium channel
xdhAB	xanthine dehydrogenase
xylB	xylulokinase
yedP	mannosyl-3-phosphoglycerate phosphatase
yfdE	CoA:oxalate CoA-transferase
yrbG	cation:H+ antiporter

gpr	L-glyceraldehyde 3-phosphate reductase
hupE	nickel transport
isdG	heme oxygenase
katG	catalase-peroxidase
kce, lcdH	L-carnitine degradation
ldhD	D-lactate dehydrogenase
mcl, mtkA	S-malate metabolism
mdcF	malonate transporter
mmcO	copper tolerance
mylcd	malonyl-CoA decarboxylase
nit2	omega-amidase
nupNOPQ	guanosine uptake
ocd	ornithine cyclodeaminase
phnZ	2-aminoethylphosphonic acid degradation
pitA	phosphate/sulfate permease

1029

1030 **Extended Data Fig. 6**. All genes in a given genome are ordered by lowest pN/pS value to
1031 highest, with genes that are differentially distributed between offshore and coastal
1032 Pelagibacteraceae genera in Fig. 4 colored red (offshore) or black (coastal) across the genomes.
1033 pN/pS values of 0.01, 0.025, 0.05, 0.075, 0.1, and 0.25 are shown in blue. pN/pS: proportion of
1034 non-synonymous to synonymous.

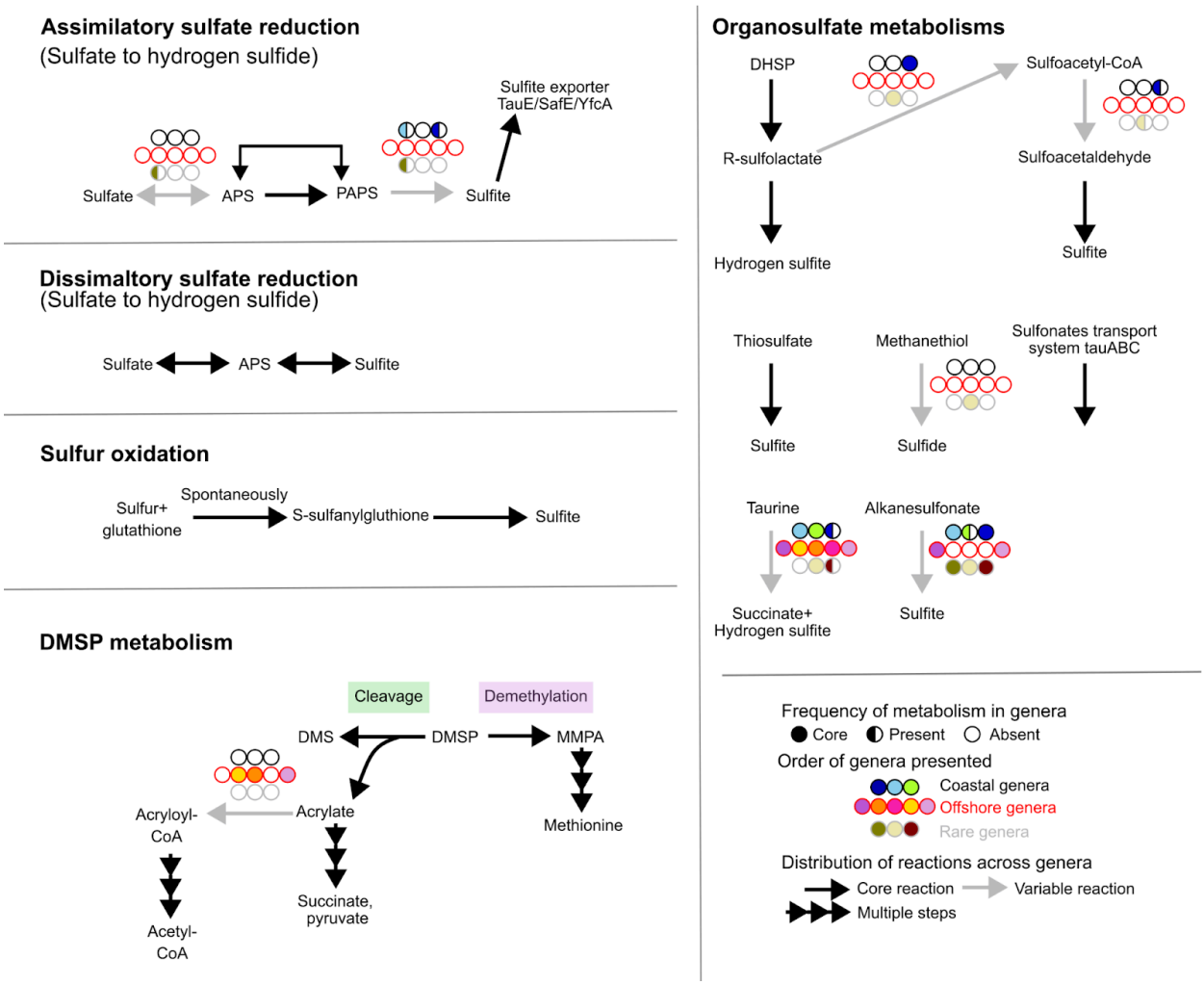

Extended Data Fig. 7. *Pelagibacteraceae* has incomplete dissimilatory and assimilatory sulfur reduction pathways and the capacity to utilize a wide diversity of organosulfate compounds. APS: adenylyl sulfate, PAPS: 3'-phosphoadenylyl sulfate, DHSP: 2,3-dihydroxypropane-1-sulfonate, DMSP: dimethylsulfoniopropionate, DMS: dimethyl sulfide, MMPA: methylmercaptopropionate, CoA: coenzyme A.

Supplementary Information

All supplementary infomation text and data files are available on Figshare at:

10.6084/m9.figshare.28087925.